

Antinucleon–nucleon/nucleus interactions studied with antiprotonic atom X-ray spectroscopy and scattering

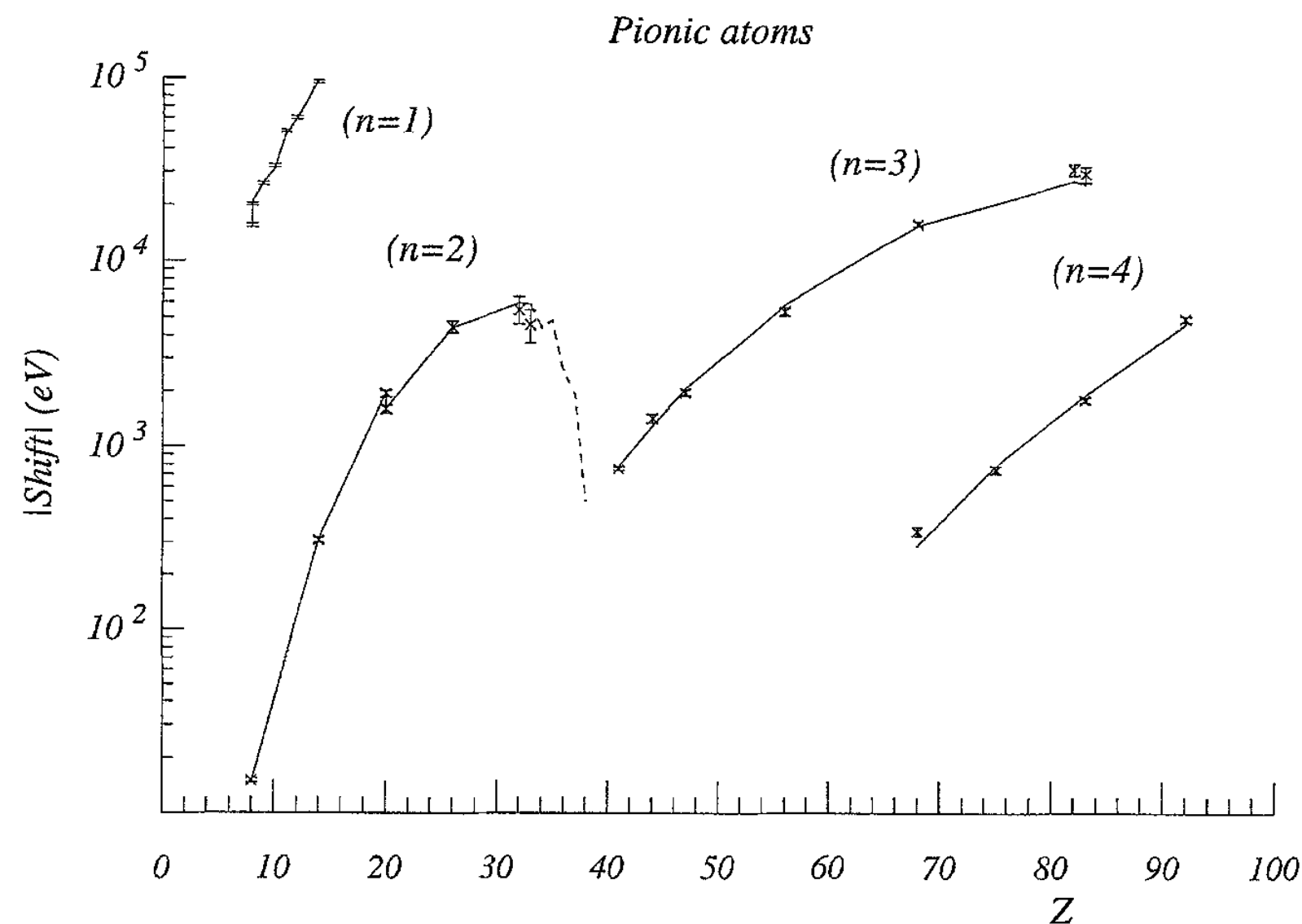
Hiroyuki Fujioka,
Institute of Science Tokyo [former TokyoTech]

Antiprotonic atom X-ray spectroscopy

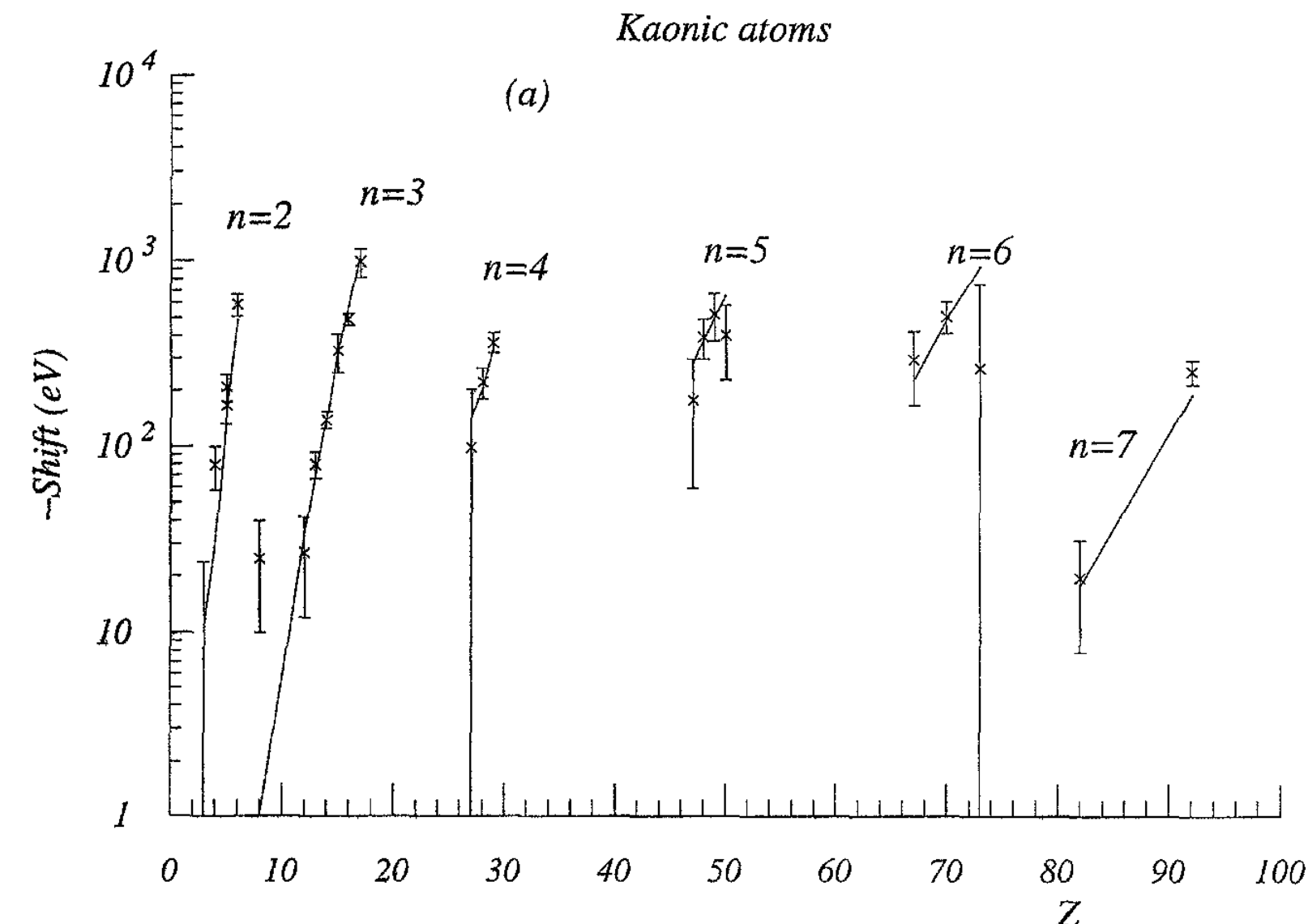
Strong interaction in exotic atoms

C.J. Batty et al., Phys. Rep. 287 (1997) 385

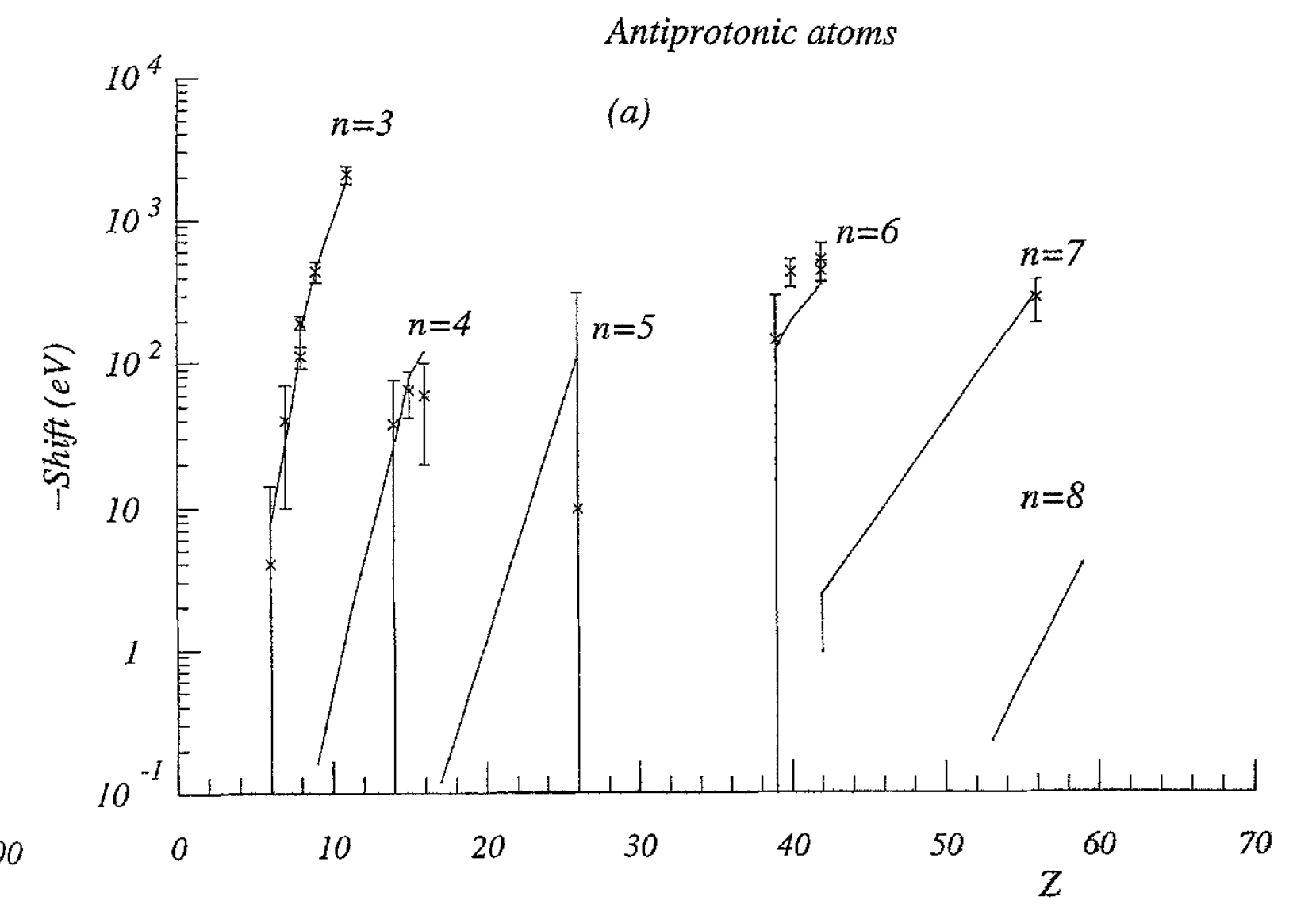
Pionic atoms



Kaonic atoms



Antiprotonic atoms



In the last three decades ...

- pionic hydrogen/deuterium
- deeply bound pionic atoms

- kaonic hydrogen/deuterium
- kaonic helium-3/4

- protonium
- anti-protonic deuterium
- **CERN PS209 (^{16}O , ..., ^{238}U)**

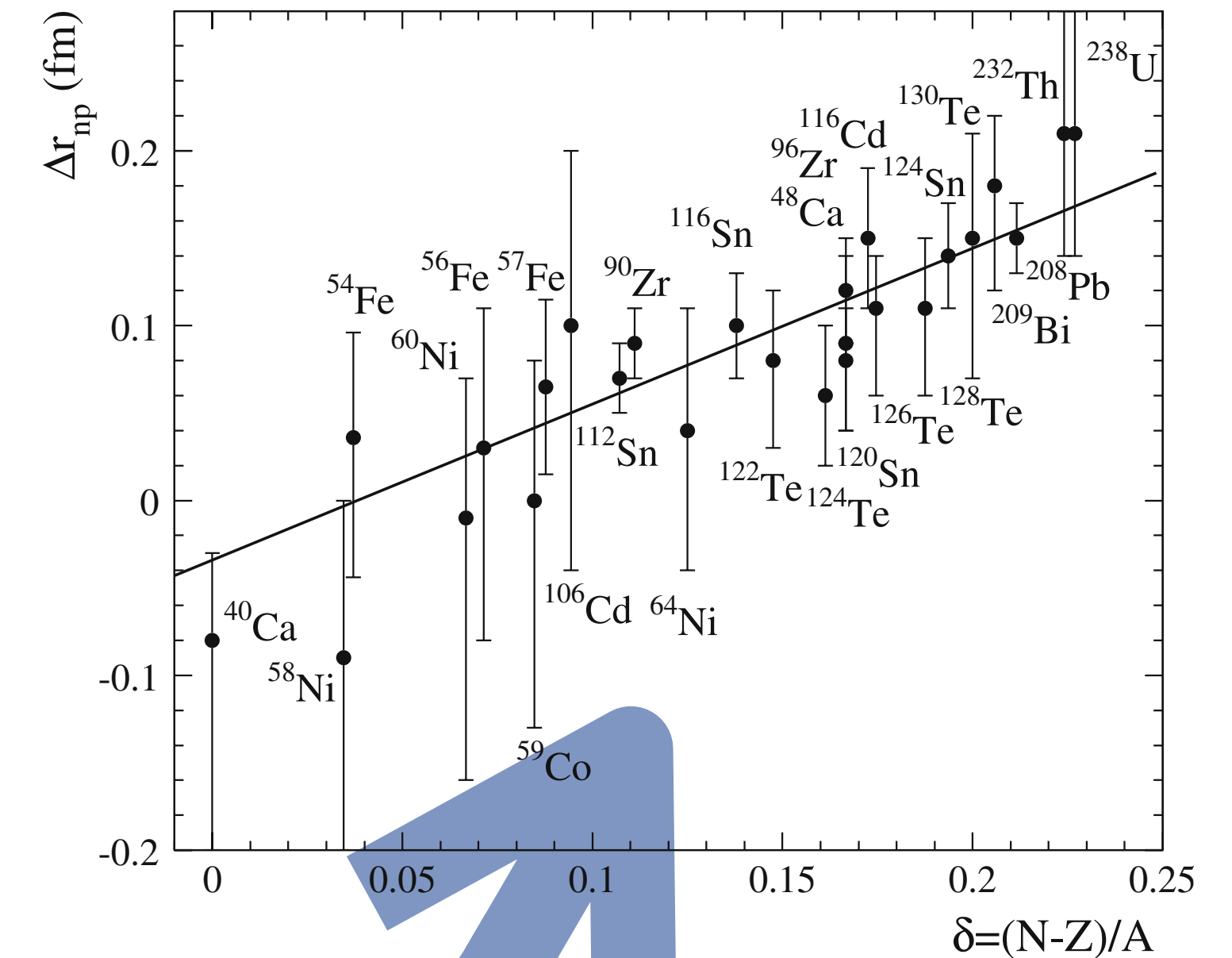
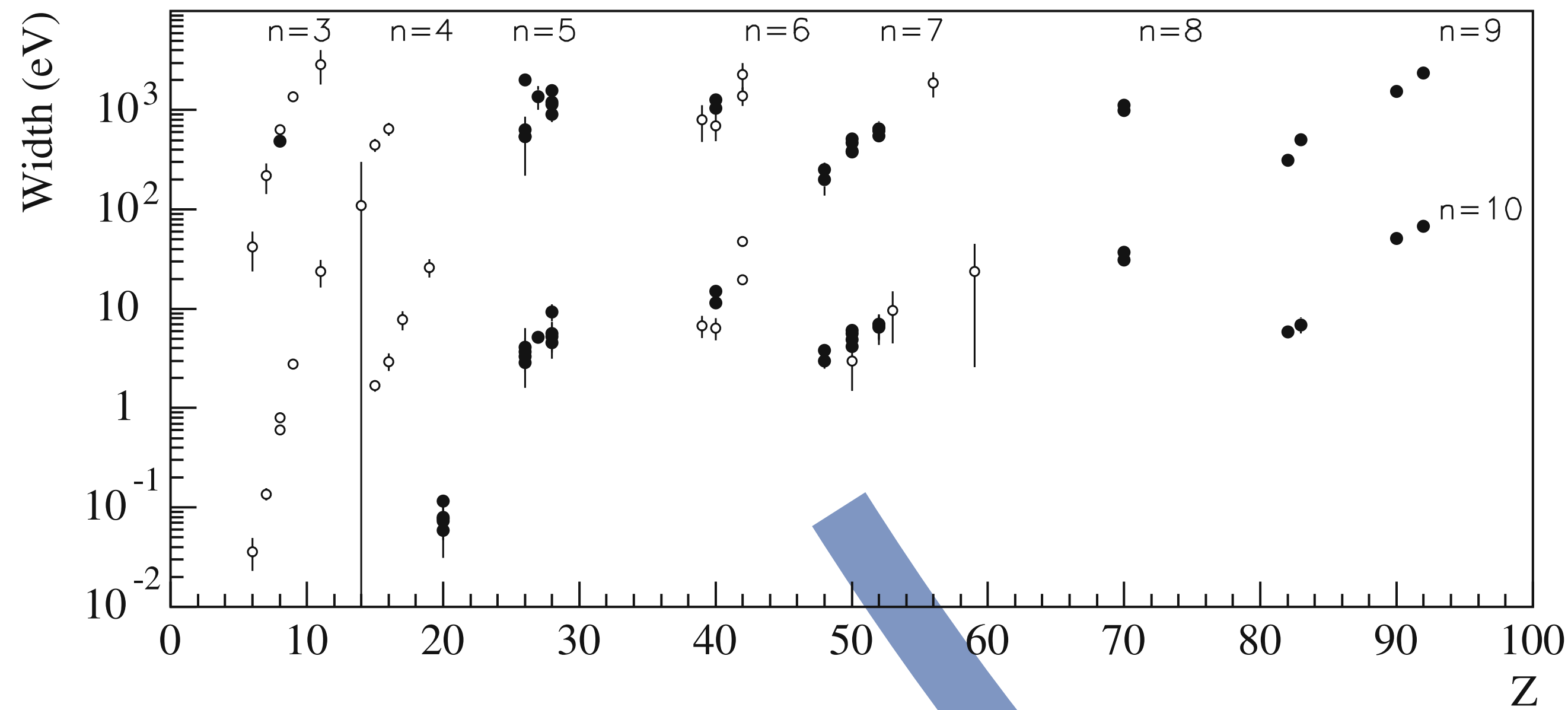
shift ($E_{\text{measured}} - E_{\text{Coulomb}}$) and width of atomic levels

⇒ strong interaction between the orbiting hadron and the core nucleus

CERN PS209 (investigation of nuclear periphery)

A. Trzcińska et al., Hyperfine Interact. 194 (2009) 271

neutron skin thickness $\Delta r_{np} = \langle r^2 \rangle_n^{1/2} - \langle r^2 \rangle_p^{1/2}$



optical potential

$$2\mu U_{\text{opt}}(r) = -4\pi \left(1 + \frac{\mu}{m} \right) (b_0 \rho(r) + b_1 \delta\rho(r))$$

$$\rho(r) = \rho_n(r) + \rho_p(r)$$

$$\delta\rho(r) = \rho_n(r) - \rho_p(r)$$

$$\rho_{n/p}(r) = \frac{\rho_0}{1 + \exp[(r - c_{n/p})/a_{n/p}]}$$

with $c_n = c_p$

$$b_0 = 2.5 + 3.4i \text{ (global fit)}$$

C.J. Batty et al., Nucl. Phys. A 592 (1995) 487

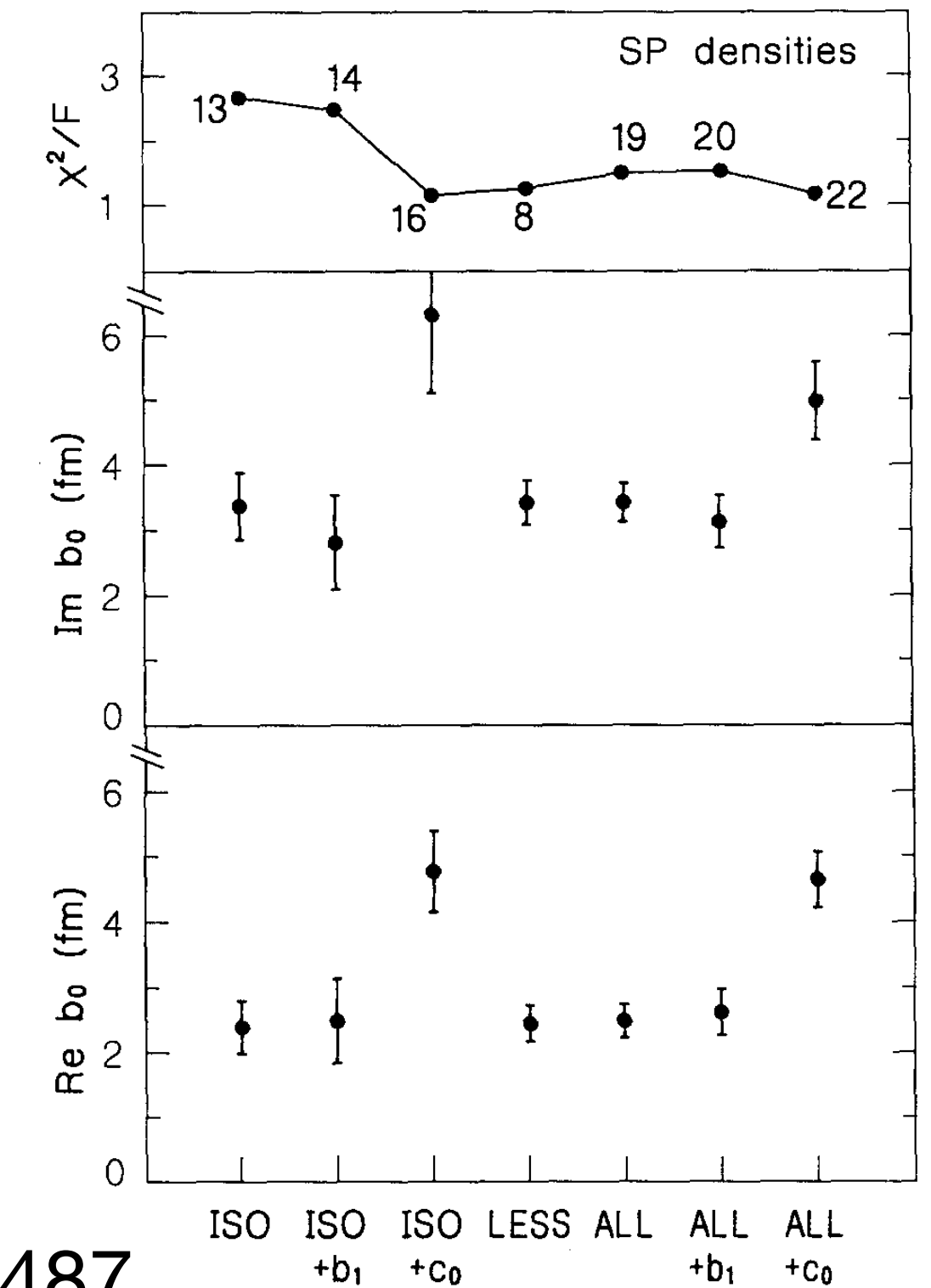
Revisiting the isovector term

$$2\mu U_{\text{opt}}(r) = -4\pi \left(1 + \frac{\mu}{m} \right) (b_0 \rho(r) + \cancel{b_1 \delta \rho(r)})$$

b_0 only

b_0, b_1

- Inclusion of **the isovector (b_1) term** did not improve the χ^2/ndf in the global fit.
- Many literatures ignores the isovector term.
- Levels are sensitive only to extremely outer, low density ($<0.1 \rho_0$) regions, where neutrons dominate over protons.



C.J. Batty et al., Nucl. Phys. A 592 (1995) 487

see also

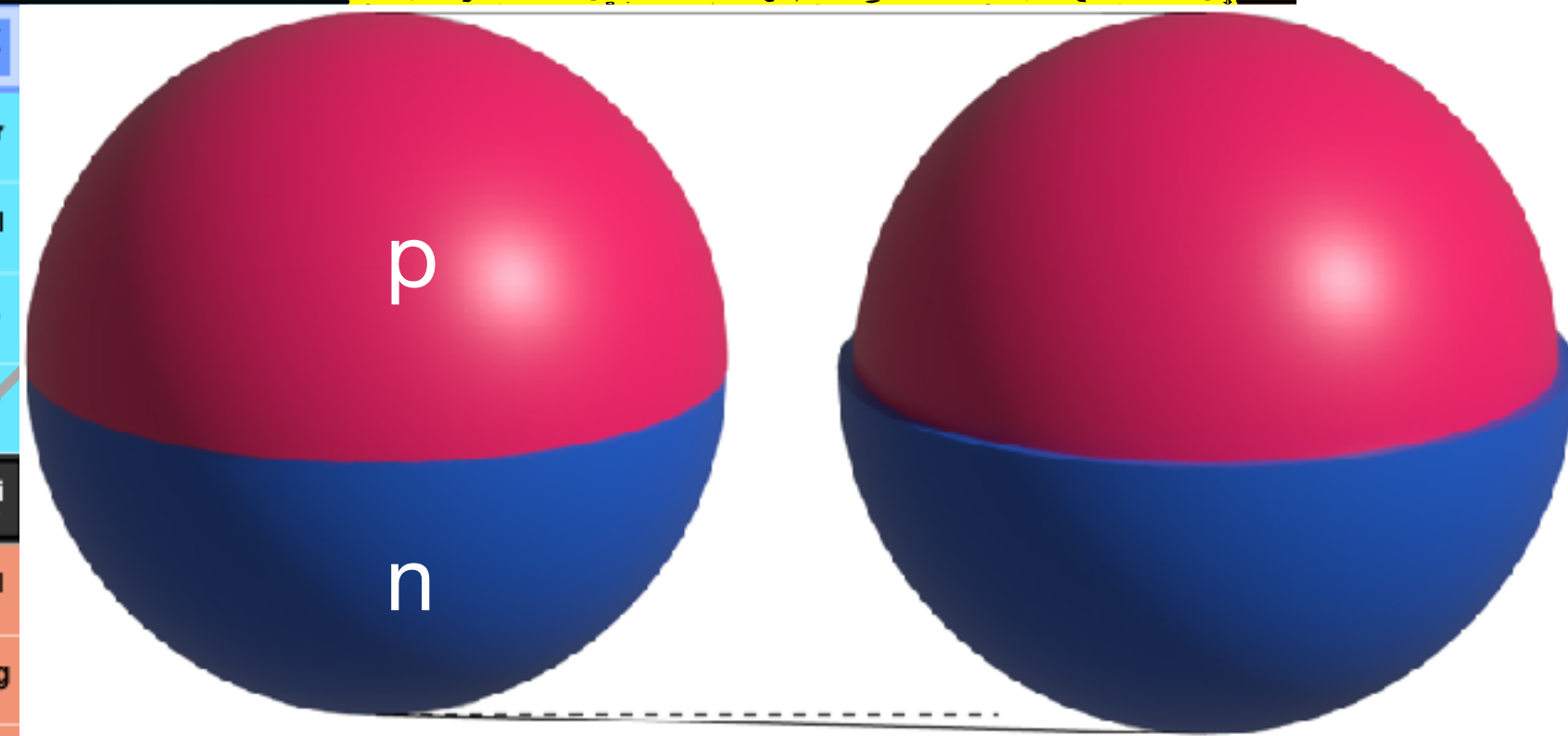
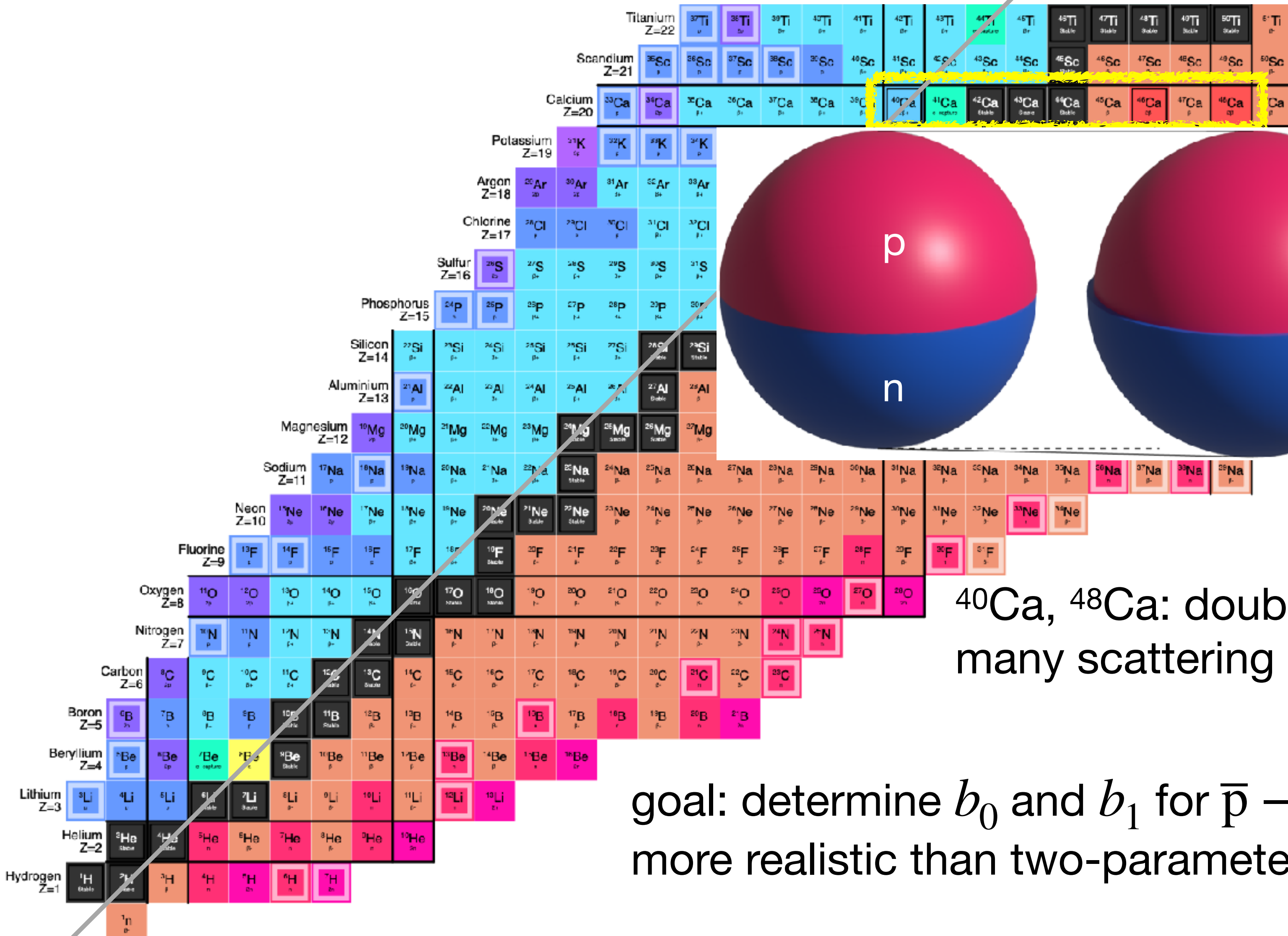
E. Friedman and A. Gal, NIM B 214 (2004) 160

E. Friedman et al., Nucl. Phys. A 761 (2005) 283

Precision Spectroscopy of antiprotonic calcium

$$N = Z$$

The last, longest stable isotope chain starting from an $N = Z$ nucleus

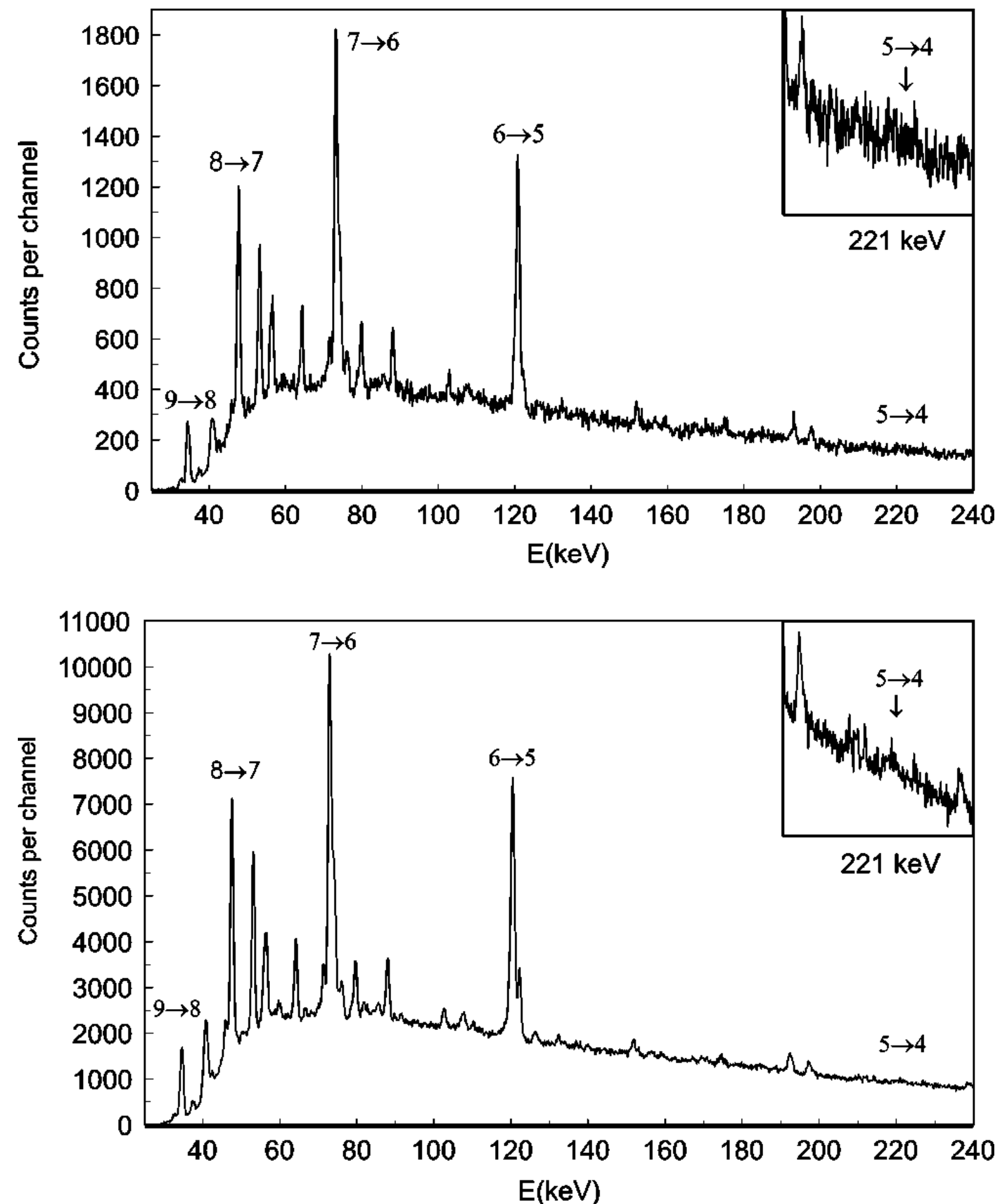


neutron skin of ^{48}Ca : $\sim 0.1\text{fm}$

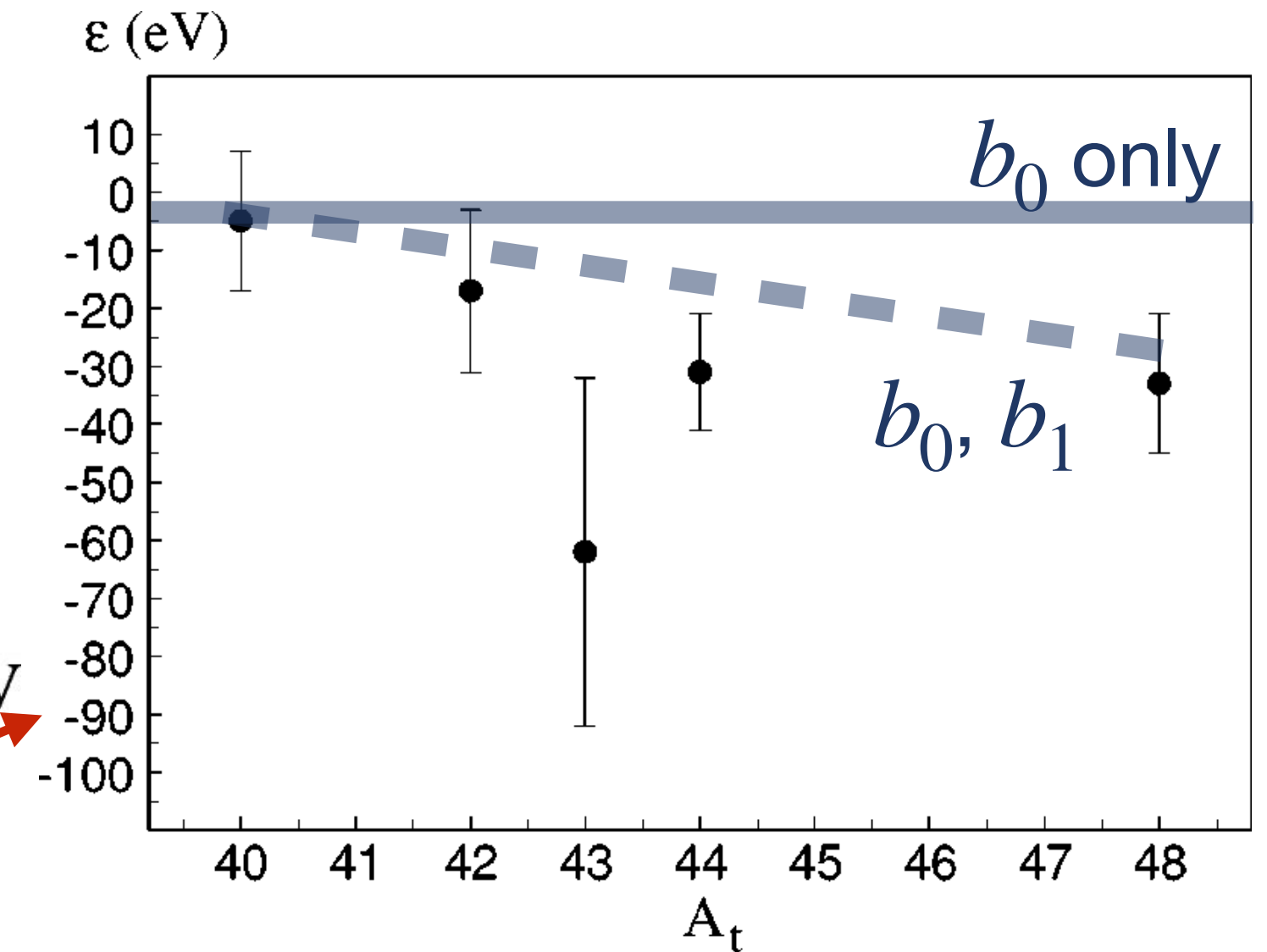
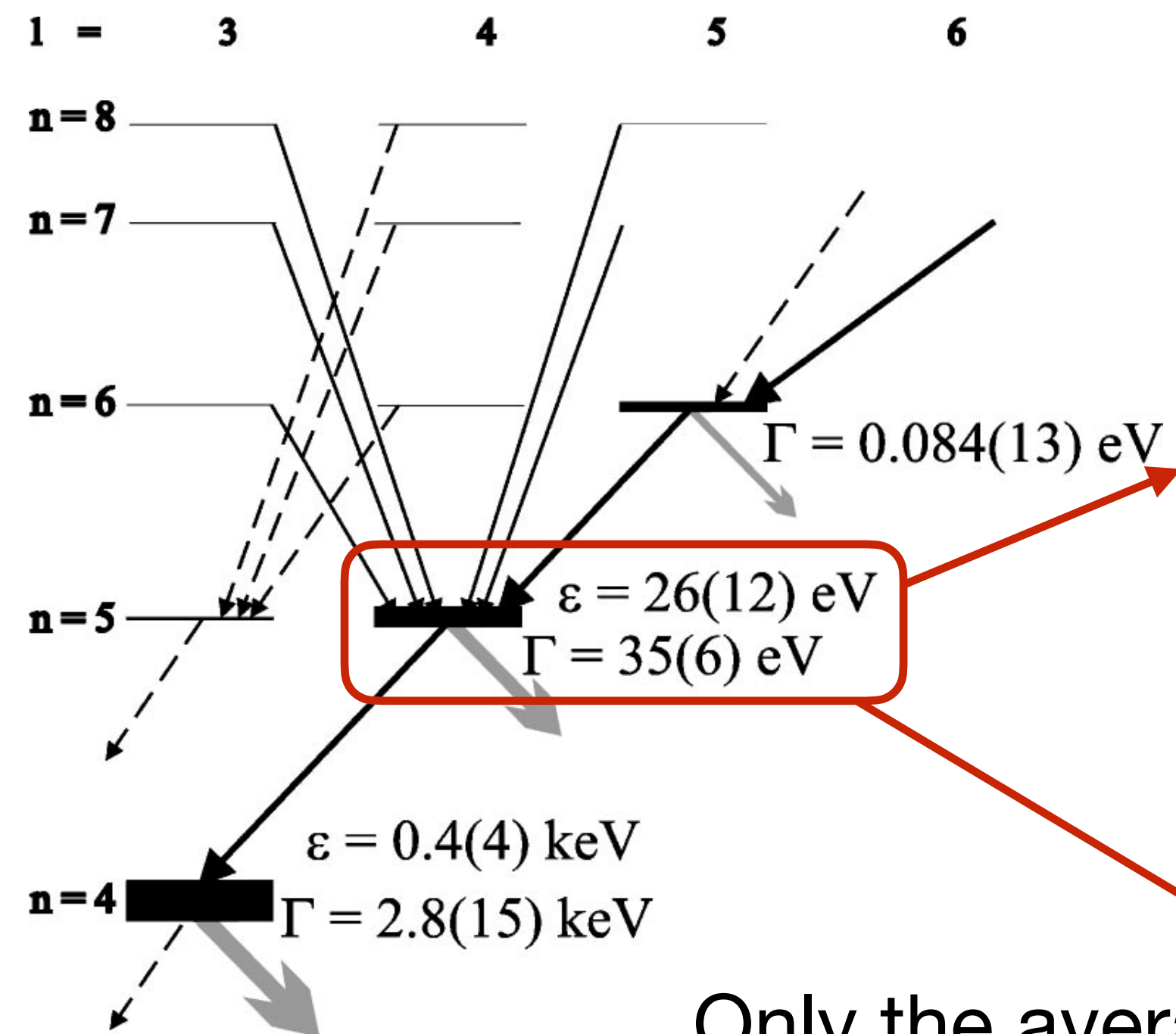
^{40}Ca , ^{48}Ca : doubly magic nuclei
many scattering experiments, structure calculations

goal: determine b_0 and b_1 for $\bar{p} - \text{Ca}$ system using nuclear densities,
more realistic than two-parameter Fermi distributions.

Closer look at PS209 calcium results



weighted average for $^{40-48}\text{Ca}$

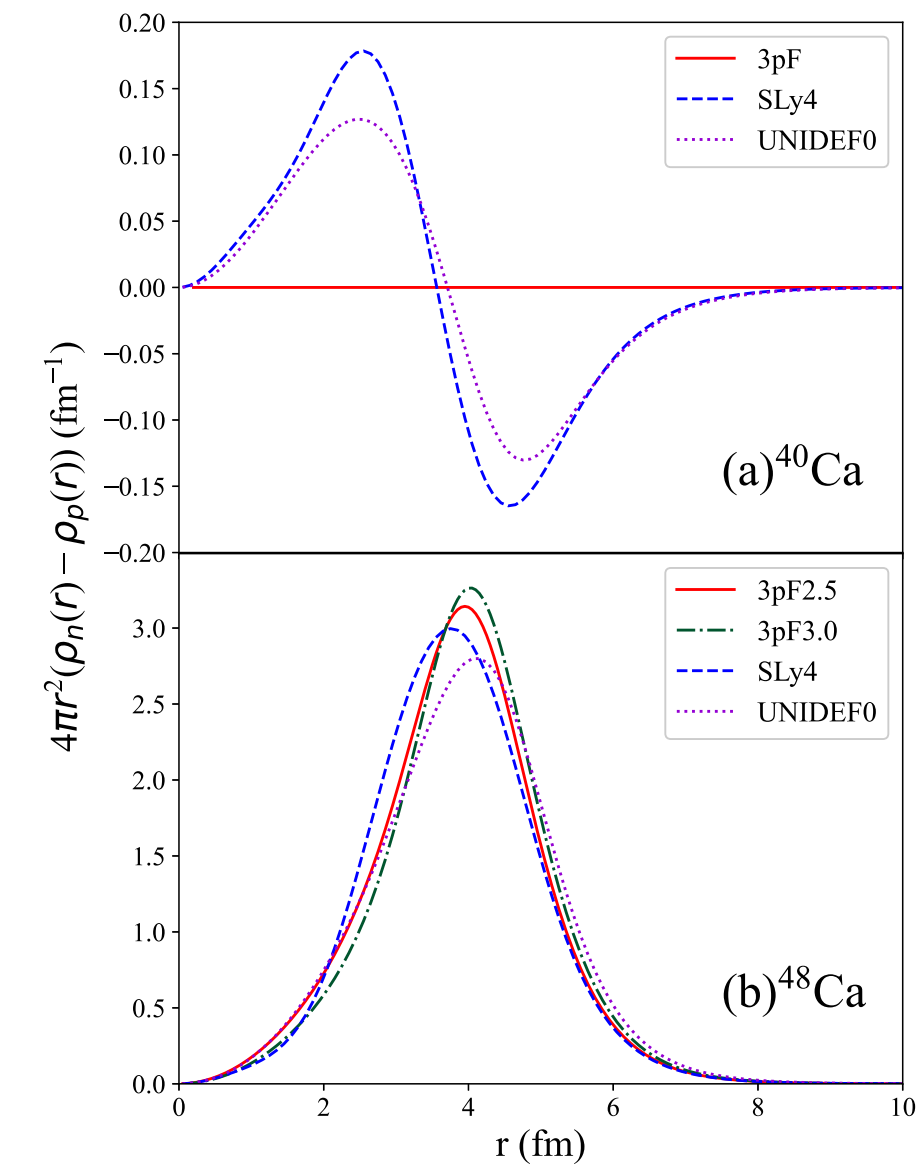


Only the averaged width was deduced.
How about mass-number dependence?

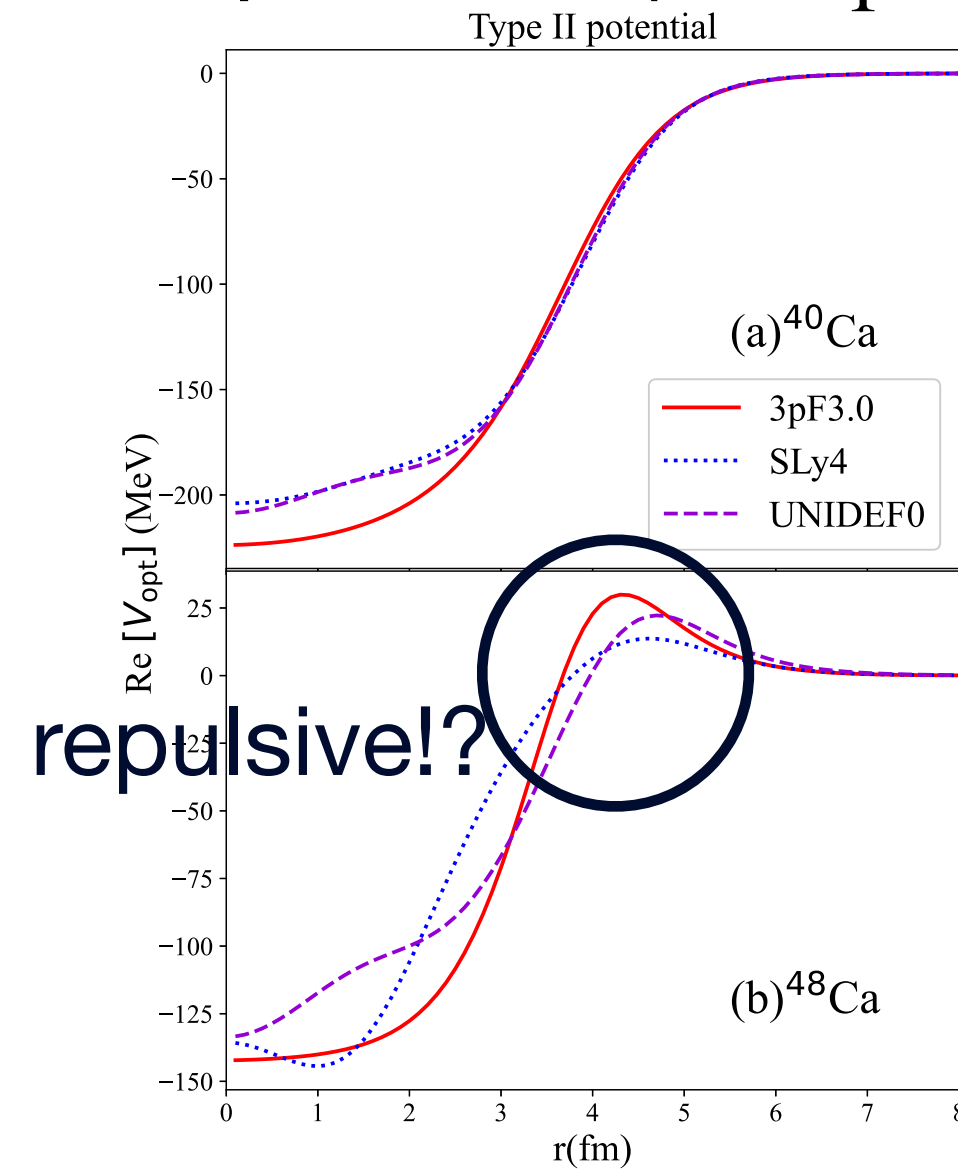
FIG. 1. Spectra of antiprotonic x rays from calcium. Upper part: spectrum from ^{48}Ca . Lower part: accumulated spectrum of all targets; the weights of the different calcium isotopes are for ^{40}Ca : 27%, ^{42}Ca : 18%, ^{43}Ca : 3%, ^{44}Ca : 24%, and for ^{48}Ca : 28% (determined from the number of antiprotons per isotope given in Table I).

Up-to-date theoretical calculation

isovector density



optical potential (w/ b_1 term)



K. Yoshimura, S. Yasunaga, D. Jido,
J. Yamagata-Sekihara, S. Hirenzaki,
arXiv:2408.14760

A large $|b_1|$ ($\text{Re}(b_0 + b_1) < 0$)
to account for the $^{40}\text{Ca} - ^{48}\text{Ca}$ difference

TABLE V. The strong shift for $n = 5$ and level width for $n = 6$ in a unit of eV, with respect to optical parameter sets. The second to the third column, the result of ^{40}Ca is provided, for the 3pF density. The fourth to fifth column exhibit the counterpart of ^{48}Ca with the 3pF-3.0 density. At the bottom line the experimental result[54] is shown.

TABLE I. The optical potential parameter sets used in this work.

	$b_0(\text{fm})$	$b_1(\text{fm})$	$c_0(\text{fm}^3)$
Type I	$2.5 + 3.4i$	–	–
Type II	$2.5 + 3.4i$	$-14.0 + 5.0i$	–
Type III	$2.5 + 3.4i$	–	$-4.0 - 2.5i$

	^{40}Ca		^{48}Ca	
	$\epsilon_{n=5}$	$\Gamma_{n=6}$	$\epsilon_{n=5}$	$\Gamma_{n=6}$
Type I	2.85	0.121	3.56	0.170
Type II	2.85	0.121	22.5	0.165
Type III	25.9	0.058	31.1	0.063
Exp.	5(12)	0.059(18)	33(12)	0.116(17)

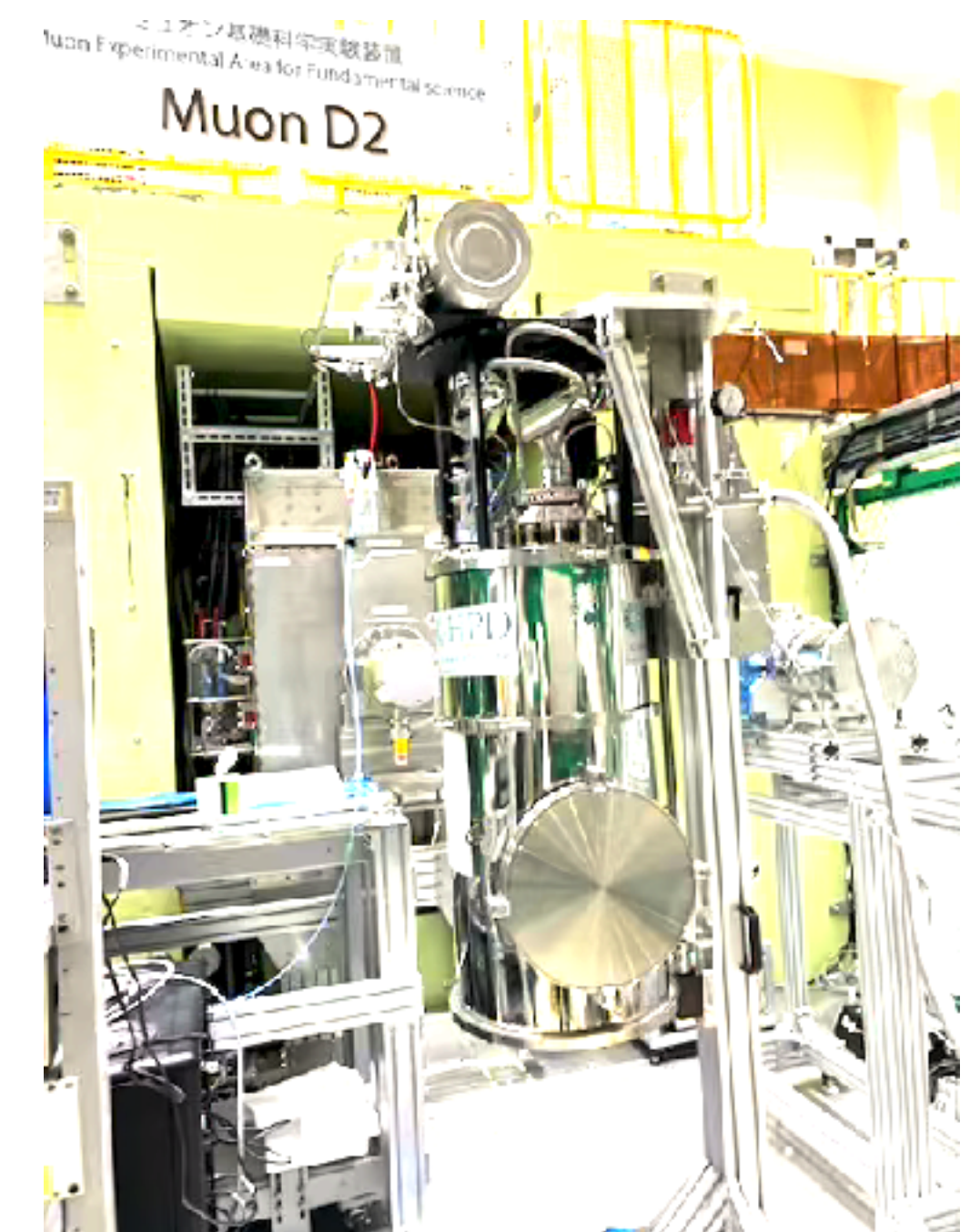
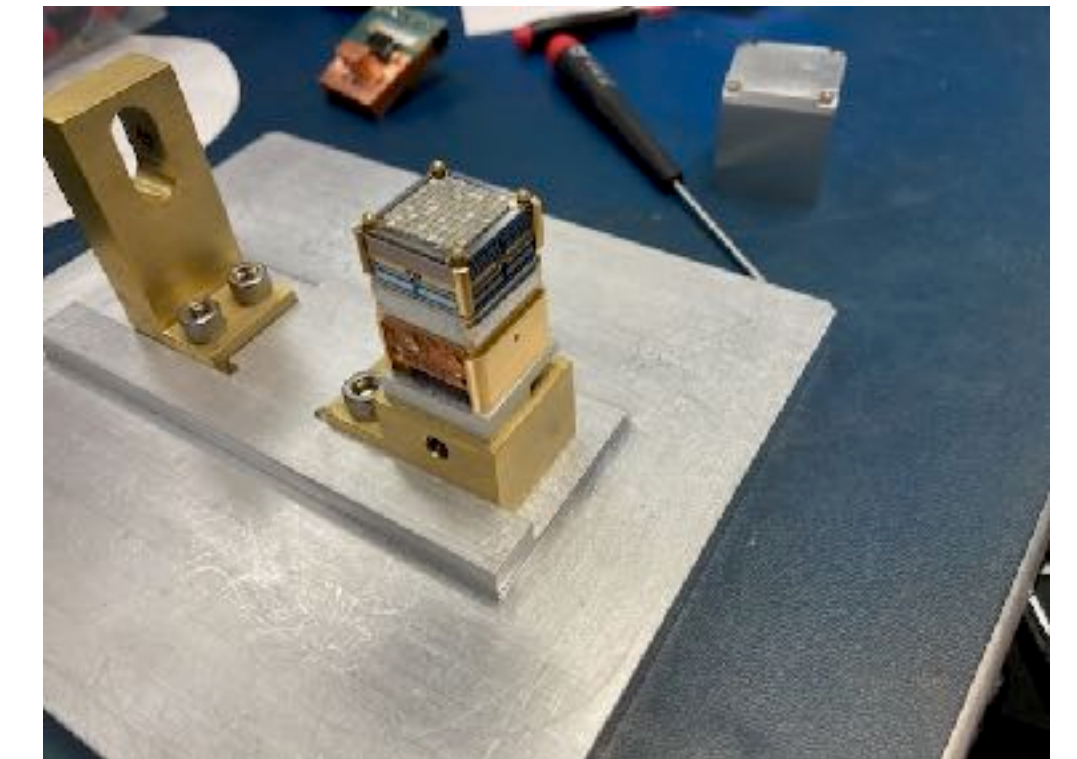
An idea of a new experiment at CERN ELENA

- Use a transition edge sensor (TES) detector instead of a HPGe detector
 - TES was used for precision spectroscopy of kaonic atoms and muonic atoms.

T. Hashimoto et al., Phys. Rev. Lett. 128 (2022) 112503

T. Okumura et al., Phys. Rev. Lett. 130 (2023) 173001

- expected resolution
 - ~ several tens eV for 120 keV X rays.



new antineutron beamline at AD

Novel concept for low-energy antineutron production and its application for antineutron scattering experiments

Alessandra Filippi,¹ Hiroyuki Fujioka,^{2,*} Takashi Higuchi,^{3,†} and Luca Venturelli^{4,5}¹INFN, Sezione di Torino²Department of Physics, Institute of Science Tokyo³Institute for Integrated Radiation and Nuclear Science, Kyoto University⁴Dipartimento di Ingegneria dell'Informazione, Università degli Studi di Brescia⁵INFN, Sezione di Pavia

(Dated: March 18, 2025)

The existing data of antiproton scattering cross sections on protons and nuclei have advanced our understanding of hadronic interactions with antinucleons. However, low-energy antineutron scattering data are scarce, thereby limiting our understanding of the S -wave antinucleon–nucleon and antinucleon–nucleus interactions. We present a novel production scheme for very low-energy antineutrons that could improve this situation. This method is based on backward charge-exchange reaction ($p\bar{p} \rightarrow n\bar{n}$), reaching the minimum momentum of 9 MeV/ c , well suited to study the S -wave antinucleon–nucleon and antinucleon–nucleus interactions. Such low-energy antineutron production can be made possible in the CERN-AD with modifications to allow antiproton extraction at 300 MeV/ c .

I. INTRODUCTION

The strong interaction between hadrons, which governs both the internal structure of hadrons through quark confinement and the formation of atomic nuclei and exotic hadrons as molecular states, is described by Quantum Chromodynamics (QCD). Because of the non-perturbative nature of the low-energy QCD, phenomenological approaches with a one-boson-exchange potential for baryon–baryon interactions have been widely applied. Recently, significant advancements have been made in QCD-based approaches, including Chiral Effective Field Theory (Chiral EFT) and Lattice QCD. Chiral EFT is based on chiral symmetry and its spontaneous breaking in the low-energy QCD regime. It describes baryon–baryon interactions using as parameters low-energy constants (LECs) [1], which are obtained by fits to experimental data. On the other hand, lattice QCD numerically simulates QCD on a discretized space-time lattice starting from first principles [2]. On the experimental side, while two-body scattering has long been used to deduce hadron–hadron interaction properties, the femtoscopy technique in proton–proton or heavy-ion collisions has emerged as a powerful tool. By combining experimental and theoretical methods, a better description of hadron–hadron interactions and their underlying mechanisms can be pursued.

Among various hadron–hadron interactions, antinucleon–nucleon ($\bar{N}N$) interactions involve annihilation dynamics, and have played a unique role in deepening our understanding of the strong interaction.

A. Antinucleon-nucleon interaction

The $\bar{N}N$ potential in a one-boson-exchange potential picture is obtained by the G -parity transformation of the NN potential, that is equivalent to change the sign of the contribution of odd G -parity boson exchange [3, 4]. As a result, the $\bar{N}N$ potential is more attractive on average than the NN potential. In particular, the ω -exchange term, which is responsible for a part of the repulsive core in the NN interaction, turns to be attractive for the $\bar{N}N$ interaction. However, for the short-range part, a complex potential should be supplemented to take into account absorptive effects in the $\bar{N}N$ annihilation. This short-range interaction must be empirically determined using $\bar{N}N$ scattering data. Several types of optical models, such as Paris potential [5], Dover–Richard potential [6, 7], and Kohno–Weise potential [8], were proposed in 1980s. These different $\bar{N}N$ models are compared in Ref. [9].

Experimental studies of $\bar{N}N$ scattering and annihilation were mostly performed during the operation of Low Energy Antiproton Ring (LEAR) (1983–1996), that leveraged ultra-slowly extracted antiproton beams spanning a wide range of momenta between 105 and 2000 MeV/ c [3, 4]. Cross sections of $\bar{p}p$ elastic scattering, charge-exchange scattering ($\bar{p}p \rightarrow \bar{n}n$), annihilation into mesons, as well as polarization observables, were measured with antiproton beams in various experiments. The PS201 (OBELIX) experiment [10–12] uniquely investigated $\bar{n}p$ annihilation as well, by operating a dedicated facility for antineutron beam production.

The wealth of experimental data on various reactions at the time played a crucial role in refining the $\bar{N}N$ interaction models. First, an energy-dependent partial-wave analysis (PWA) was performed [13]. The long-range interaction in the PWA was based on the one-pion and two-pion exchange contributions derived via Chiral EFT similarly to the nucleon–nucleon PWA, whereas the short-

R. Caravita¹, A. Cridland Mathad², J. S. Hangst³, M. Hori⁴, B. M. Latacz², A. Obertelli⁵, P. Perez⁶, S. Ulmer^{7,8*}, E. Widmann⁹on behalf of the Antiproton Decelerator User Community (ADUC)[†]¹ TIFPA/INFN Trento, Italy² CERN, Switzerland³ Aarhus Universitet, Denmark⁴ Imperial College London, United Kingdom⁵ Technische Universität Darmstadt, Germany⁶ IRFU, CEA, Université Paris-Saclay, France⁷ Heinrich-Heine-Universität Düsseldorf, Germany⁸ RIKEN, Japan⁹ Stefan Meyer Institute, Austria

April 1, 2025

Input to the European Strategy for Particle Physics - 2026 update

8 New Proposals

In addition to the long range plans highlighted within the existing experiments, new physics ideas such as antiprotonic atom X-ray spectroscopy (PAX), spectroscopy of hypernuclei (HYPER), antihydrogen molecular ion (collaboration of many groups into which members from ALPHA, GBAR, BASE, HHU, MPIK and many others will be involved), study of properties of antideuterons (AEgIS, ASACUSA, BASE, EXEQT and GBAR), collision experiments using continuous beams (ASACUSA), and low energy antineutron physics, are discussed in this section. Some of these ideas are already in the preparation phase, including successful or ongoing grant applications.

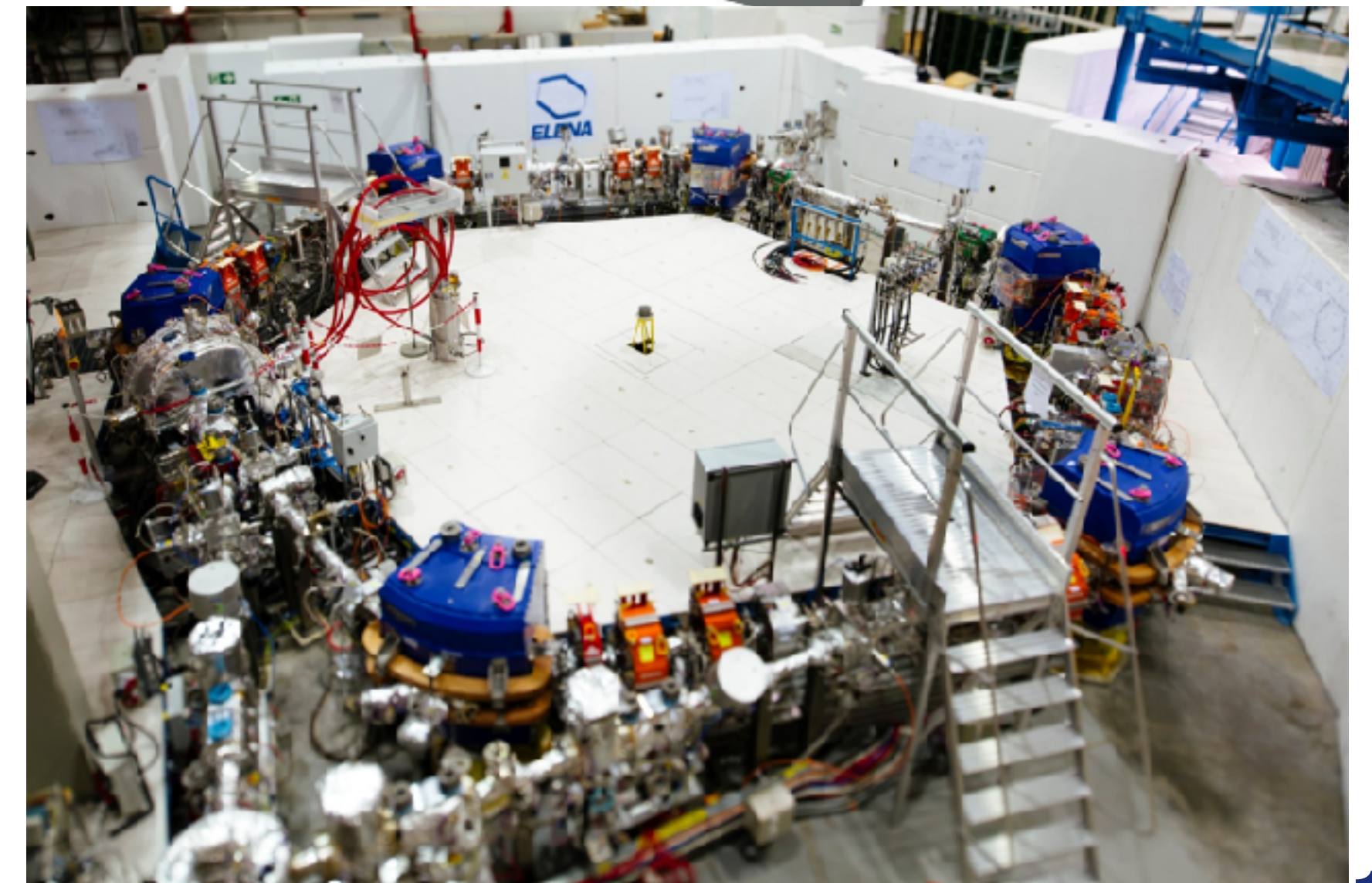
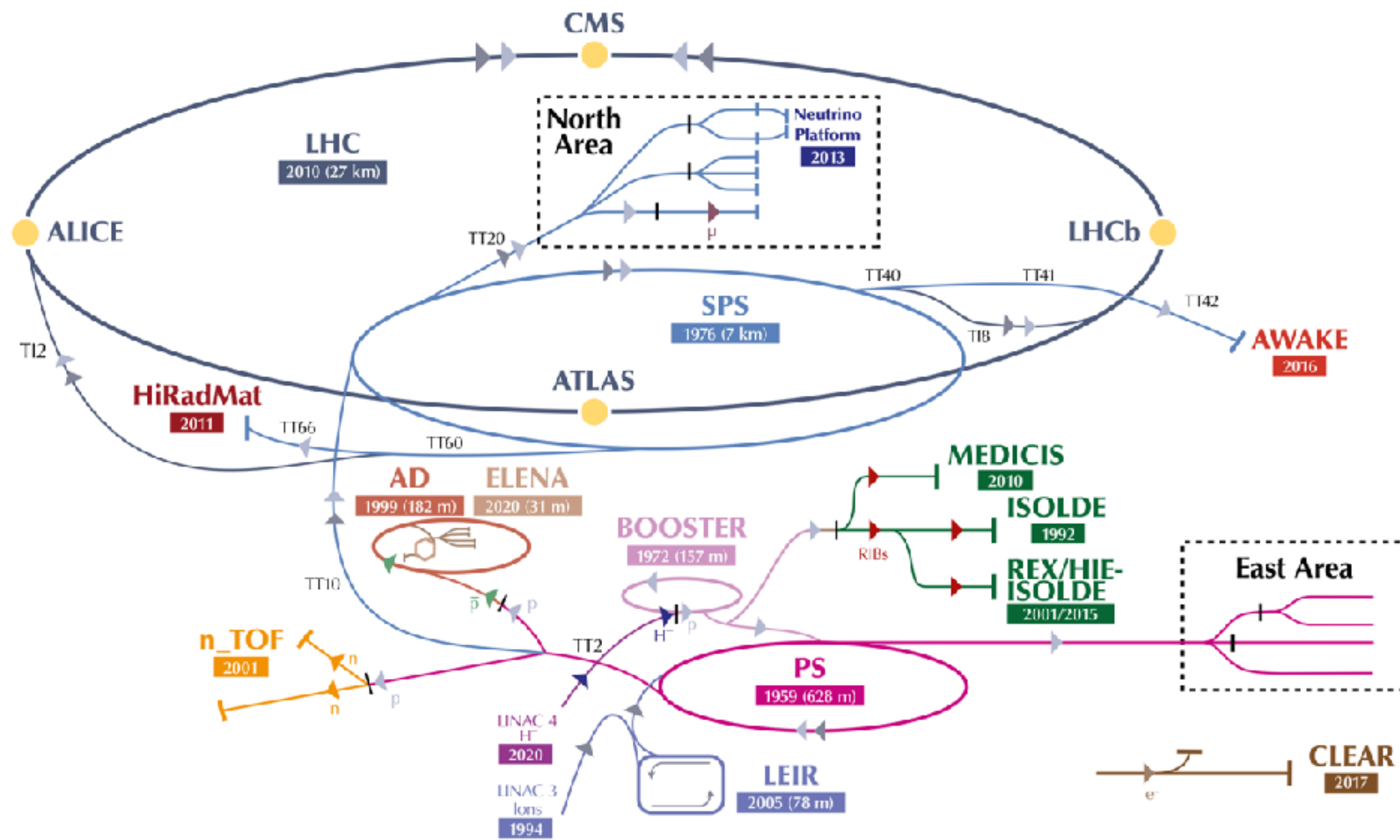
8.6 Low energy antineutrons

Antinucleon–nucleon interactions were explored at CERN-LEAR, with antineutron beams of momenta above 50 MeV/ c . Lower energy antineutrons down to 9 MeV/ c can be produced through a charge-exchange reaction ($\bar{p}p \rightarrow \bar{n}n$) with a 300 MeV/ c antiproton beam from the AD [67]. It is considered as the possibility to study unresolved problems of low-energy antineutron dynamics, and unveil the origins of a $p\bar{p}$ enhancement and X resonances near the $p\bar{p}$ threshold, as observed in the BESIII experiment.

* fujioka@phys.sci.isct.ac.jp

† higuchi.takashi.8k@kyoto-u.ac.jp

CERN AD (Antiproton Decelerator)

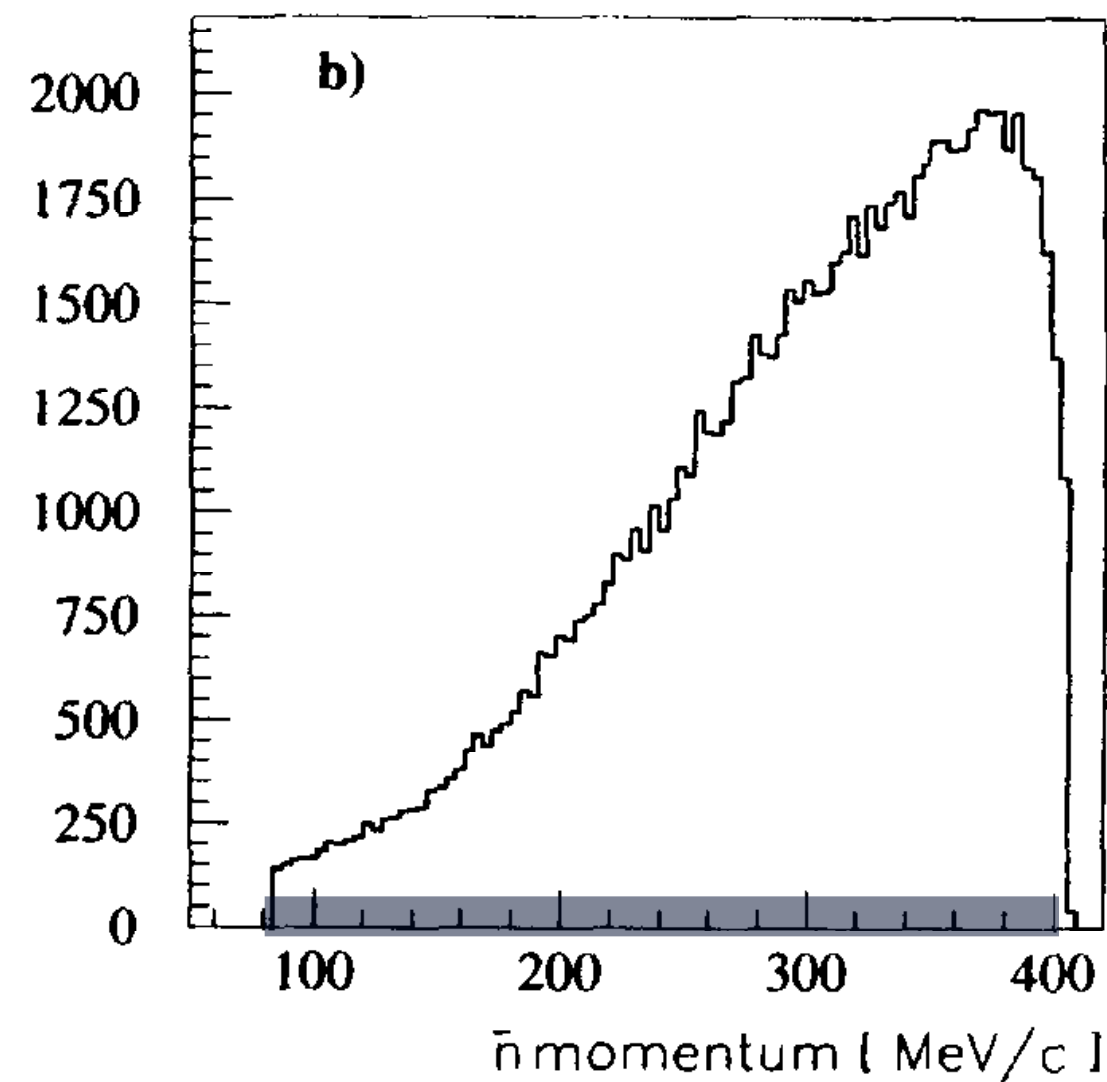


Novel concept: low-energy antineutron production

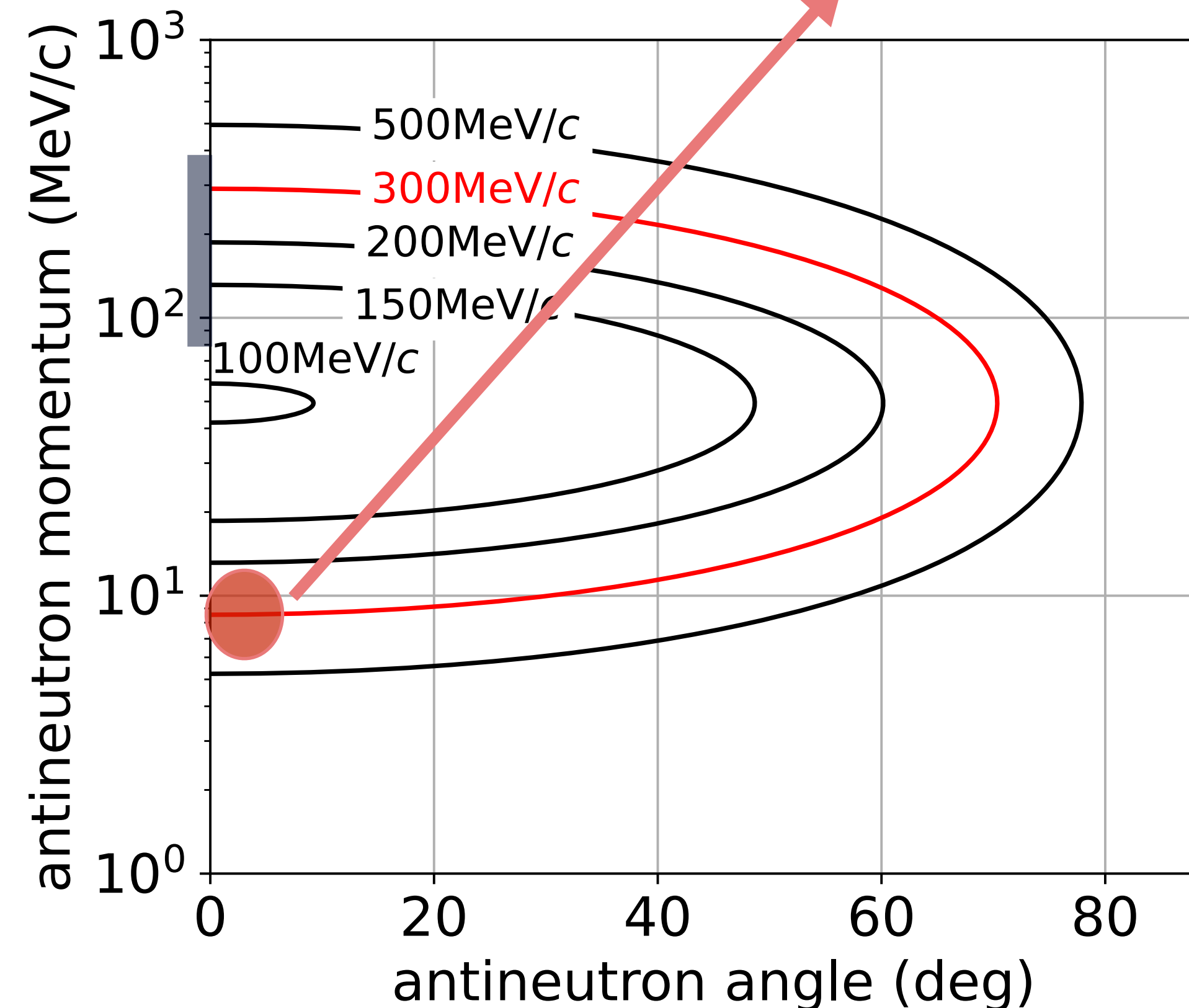
- 300 MeV/c antiprotons from CERN-AD (Antiproton Decelerator)
- **9 MeV/c or 40 keV (in lab) antineutrons** can be backward-produced in charge-exchange reaction ($p\bar{p} \rightarrow n\bar{n}$)

~1 antineutron per cycle (~ 2 min.)
⇒ sufficient for scattering experiments

OBELIX experiment

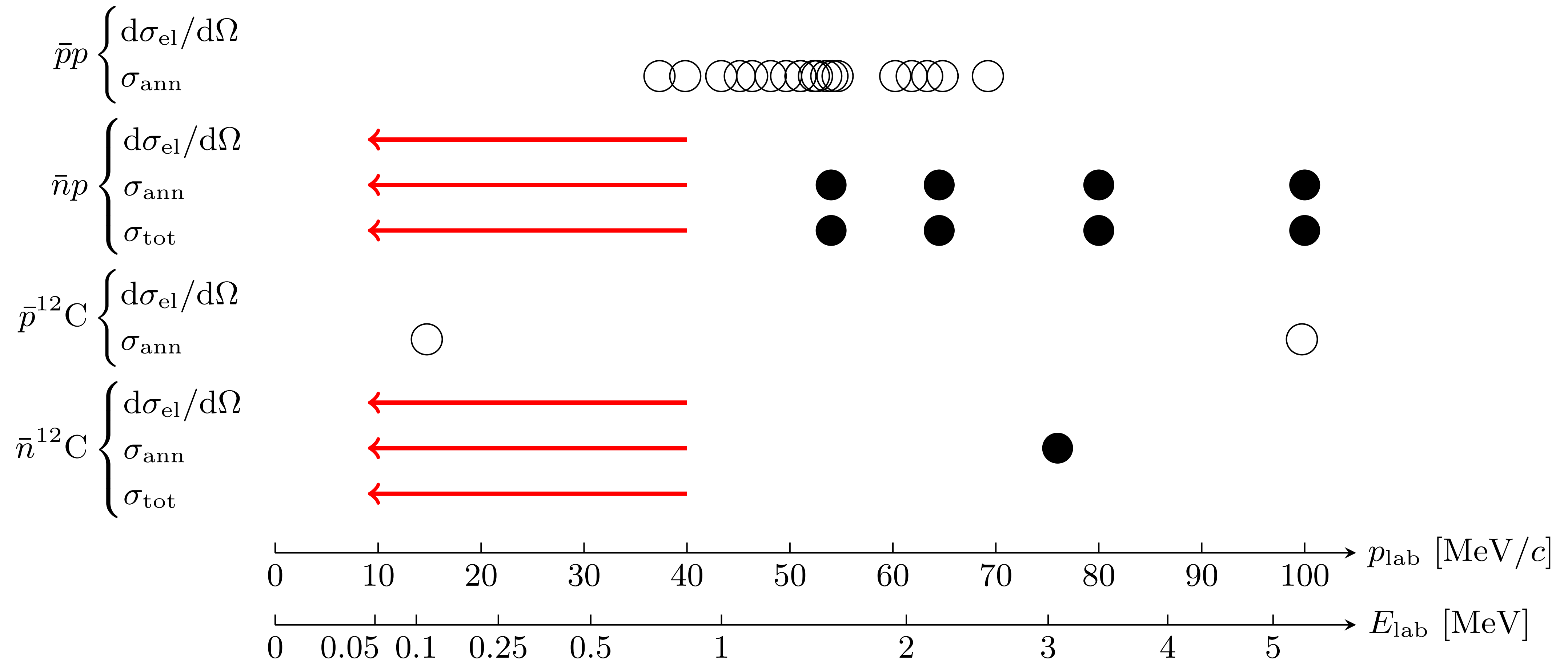


NIM A 399 (1997) 11



momentum adjustable
by inserting a beam degrader
and optimizing the dimension
of a production target of LH₂

Summary of existing data and prospect



Low-energy antineutron-proton scattering

- Only S-wave scattering is important in case of $\hbar k = p_{\text{Lab}}/2 \lesssim 25 \text{ MeV}/c$
- scattering amplitude: $f_{\ell=0} = 1/(k \cot \delta - ik)$
 - ▷ $k \cot \delta \approx -1/a \equiv \alpha = \alpha_R - i\alpha_I$ ($\alpha_I > 0$) in the low-energy limit
 - ▷ scattering length: $a = a_R - ia_I$ ($a_I > 0$)
- elastic scattering cross section: $\sigma_{\text{el}} = \frac{4\pi}{\alpha_R^2 + (\alpha_I + k)^2} \approx 4\pi |a|^2 (1 - 2a_I k)$
- annihilation cross section: $\sigma_{\text{ann}} = \frac{4\pi}{k} \frac{\alpha_I}{\alpha_R^2 + (\alpha_I + k)^2} \approx \frac{4\pi}{k} a_I - 8\pi a_I^2$

Antineutron–proton scattering

NN interaction and N \bar{N} interaction

- One-boson-exchange models

- ▷ $V_{NN} = V_{\pi} + V_{2\pi} + V_{\eta} + V_{\rho} + V_{\omega} + \dots$ (Paris potential)

↓ G-parity transformation

$$V_{N\bar{N}} = -V_{\pi} + V_{2\pi} + V_{\eta} + V_{\rho} - V_{\omega} + \dots$$

- ▷ The short-range part is replaced by an annihilation potential $V_0 + iW_0$

- NN Paris potential → N \bar{N} Paris potential

- Dover-Richard, Kohno-Weise, ...

- Partial Wave Analysis [PRC 86 (2012) 044003]

- Chiral EFT [up to N³LO, JHEP 07(2017) 078]

- no Lattice QCD calculation

- All these approaches rely on experimental data, that are more than three decades old.

Low-energy antiproton-proton scattering (annihilation)

- Due to attractive Coulomb interaction
 - ▷ $\sigma \propto \beta^{-2}$ instead of $\sigma \propto \beta^{-1}$
 - ▷ p-wave doesn't vanish even when $E \rightarrow 0$
 - ▷ Coulomb-corrected scattering length a_{sc} can be deduced as follows:

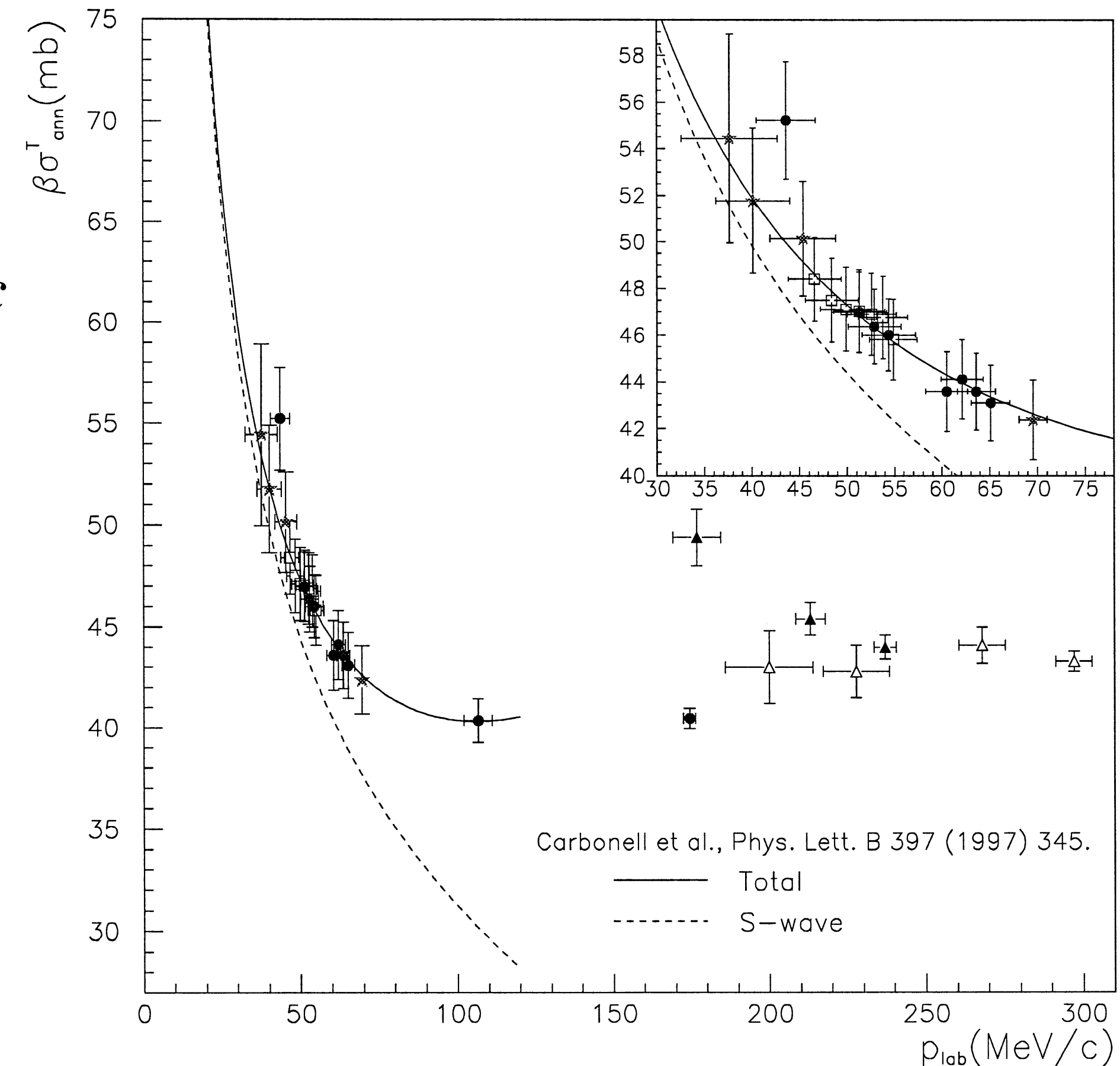
$$q^2 \sigma_{\text{ann}}^{sc} (\text{S-wave}) = \frac{8\pi^2}{1 - e^{2\pi\eta}} \frac{\text{Im}(-a_{sc}/B)}{|1 + iq w(\eta) a_{sc}|^2}, \quad (1)$$

where:

- $\eta = -1/qB$ is the dimensionless Coulomb parameter with B the $\bar{p}p$ Bohr radius;
- $w(x) = c_0^2(x) - 2ixh(x)$ is an auxiliary function with $qBw(\eta) \rightarrow 2\pi$ when $q \rightarrow 0$;
- c_0^2 and h are the usual functions in the Coulomb scattering theory

$$c_0^2(x) = \frac{2\pi x}{\exp(2\pi x) - 1};$$

$$h(x) = \frac{1}{2} [\Psi(-ix) + \Psi(ix)] - \frac{1}{2} \ln(x^2)$$



J. Carbonell et al., PLB 397 (1997) 345

A. Zenoni et al., PLB 461 (1999) 405

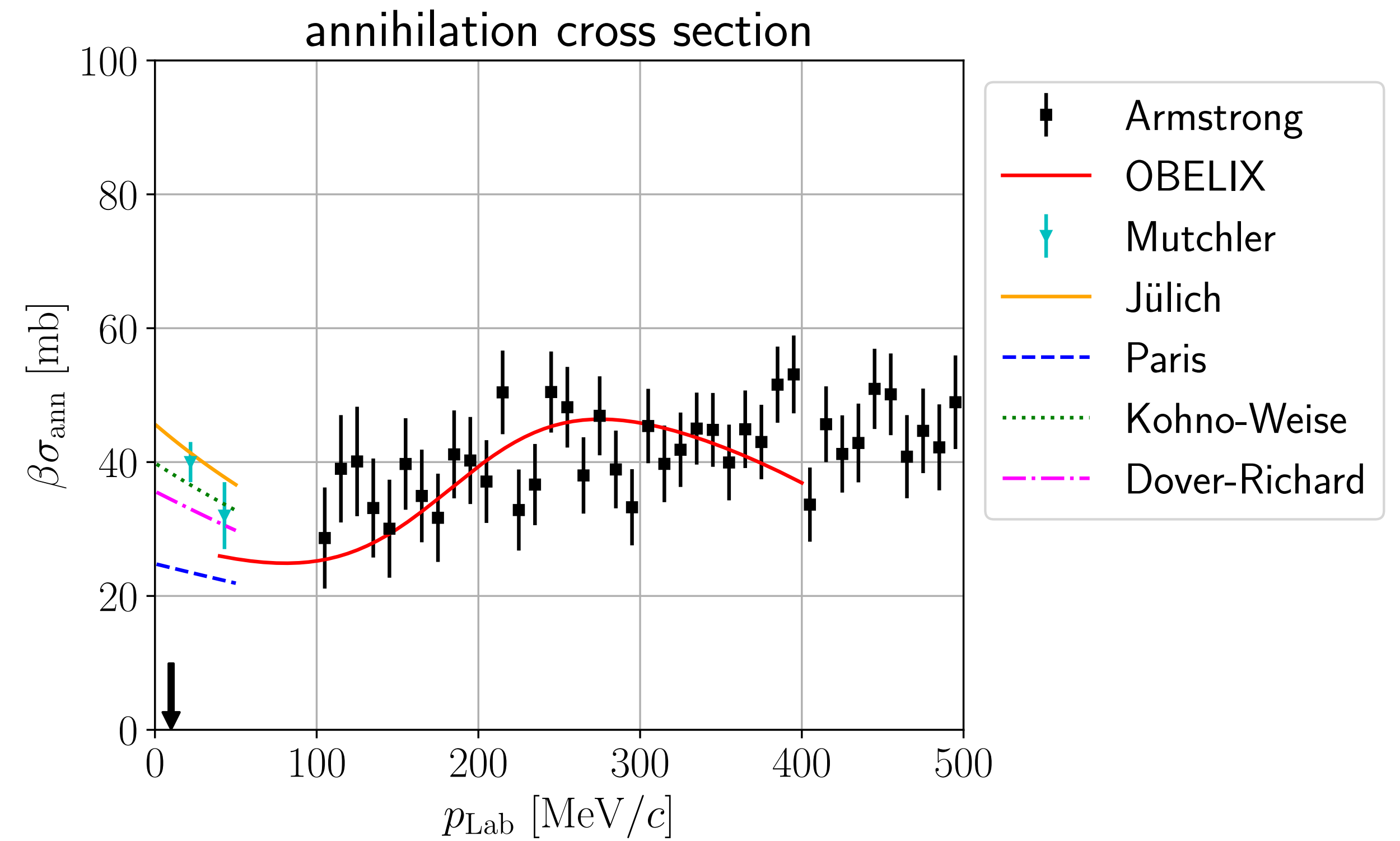
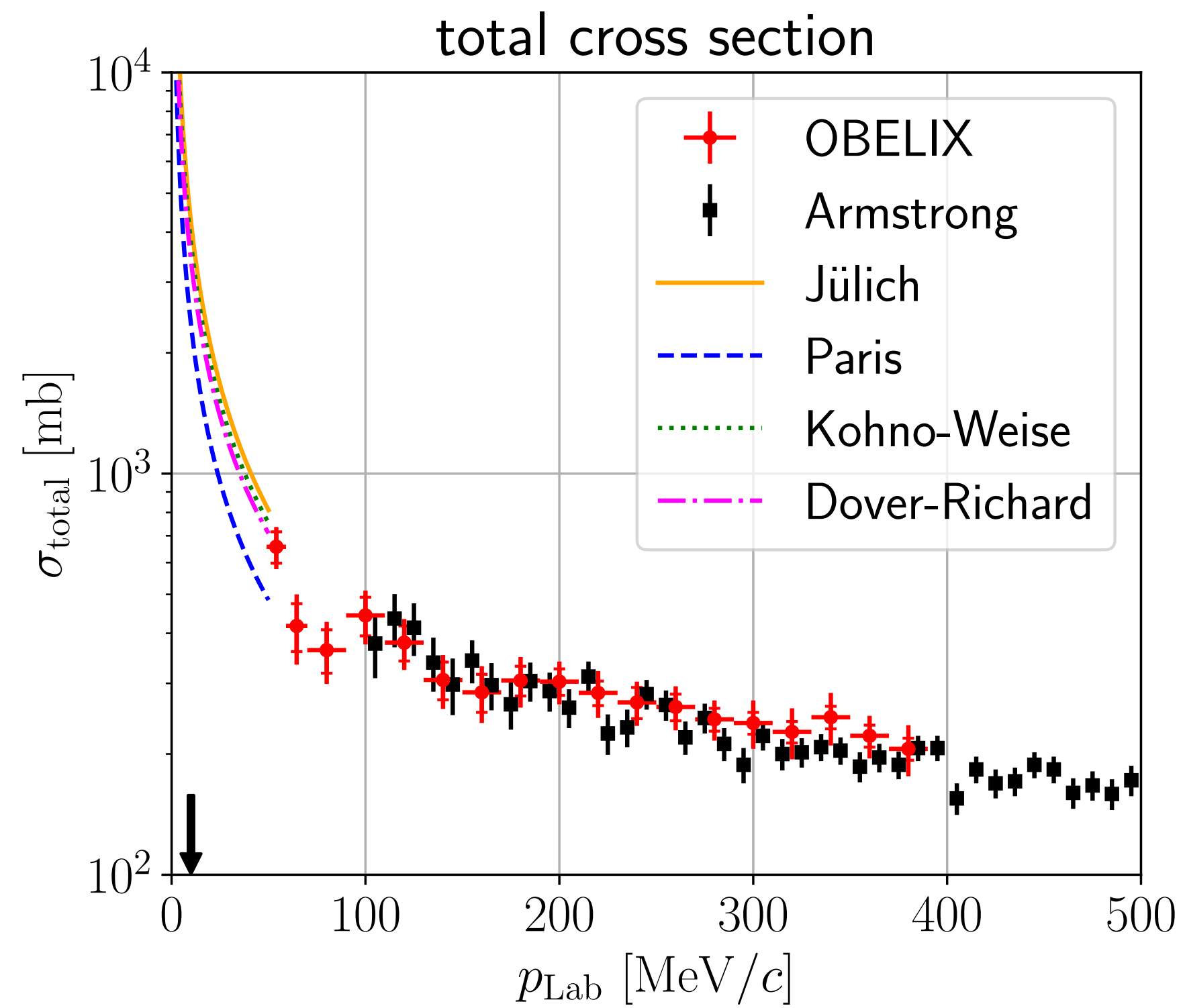
Scattering lengths in various interaction models

	a_0	r_0	a_0	r_0
T = 0	$^{11}\text{S}_0$		$^{13}\text{SD}_1$	
Nijm*	-0.17 -1.01i	-6.9-2.9 i	-	-
Jülich	-0.21 -1.23i	-	1.42-0.88i	-
Paris 09	1.27 -1.18i	-0.53+0.14i	1.20-0.80i	-
KW	-0.03-1.35i	-4.7-7.9i	1.23-0.77i	-
DR2	0.10 -1.07i	-11-6.2i	1.28-0.78i	-
T = 1	$^{31}\text{S}_0$		$^{33}\text{SD}_1$	
Nijm*	1.02 -0.60i	0.7-1.2i	-	-
Jülich	1.05 -0.58i	-	0.44-0.96i	-
Paris 09	0.76 -0.56i	0.9-3.9i	0.61-0.44i	-
KW	1.07 -0.62i	0.7-1.9i	0.78-0.80i	-
DR2	1.20 -0.57i	0.6-1.6i	0.89-0.71i	-

$\bar{p}p$ scattering

$\bar{n}p$ scattering

Previous measurements of $\bar{n}p$ scattering (1)



OBELIX: PLB 475 (2000) 378
Armstrong: PRD 36 (1987) 659

OBELIX: NPB 56A (1997) 227c
Armstrong: PRD 36 (1987) 659
Mutchler: PRC 38 (1988) 742 [antineutron 'lifetime' in Liq.H2]

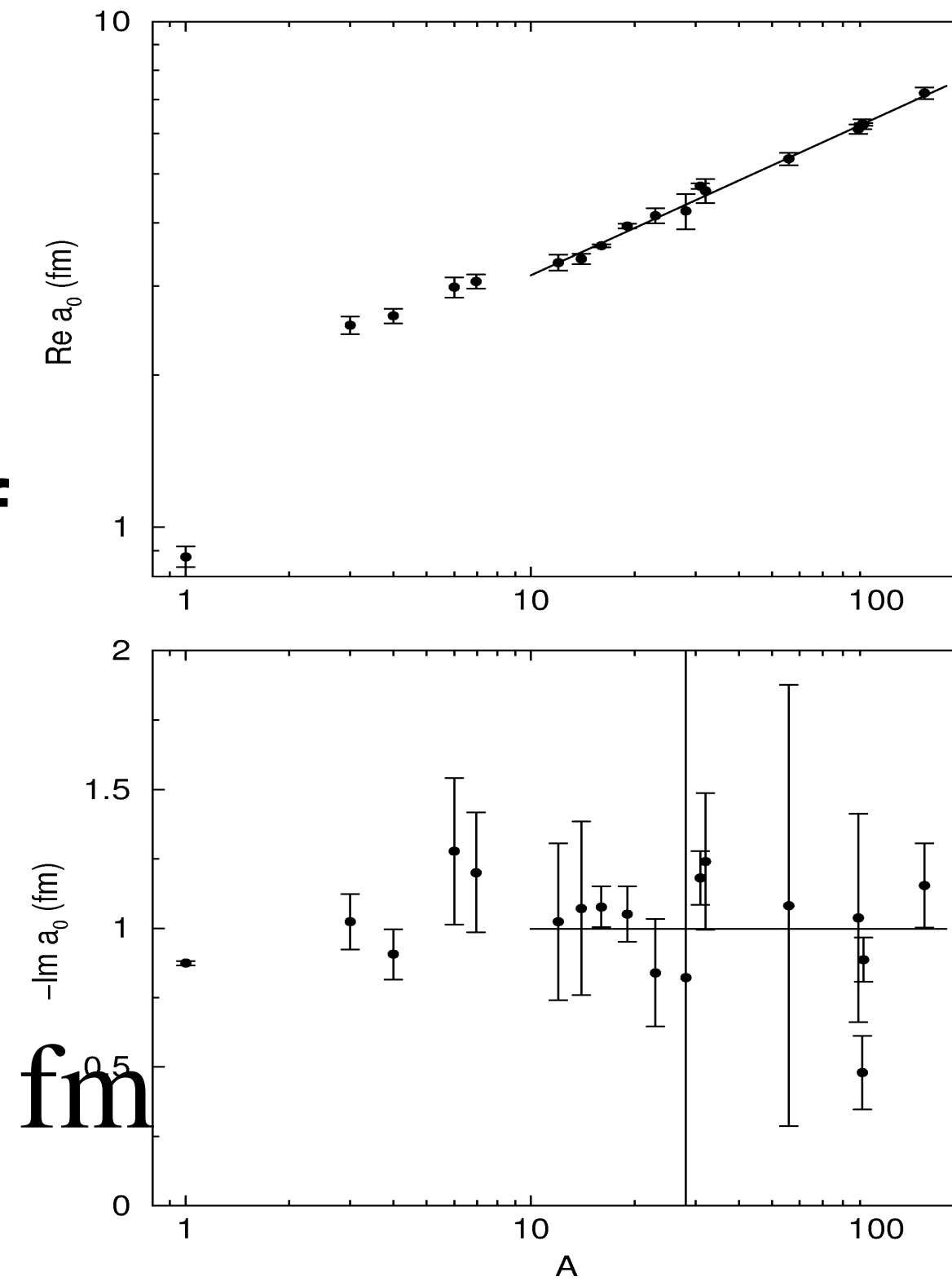
Antineutron–nucleus scattering

Antineutron-nucleus scattering lengths

- Indirectly determined by solving a Schrödinger eq. with the optical potential, which reproduces energy levels of antiprotonic atoms

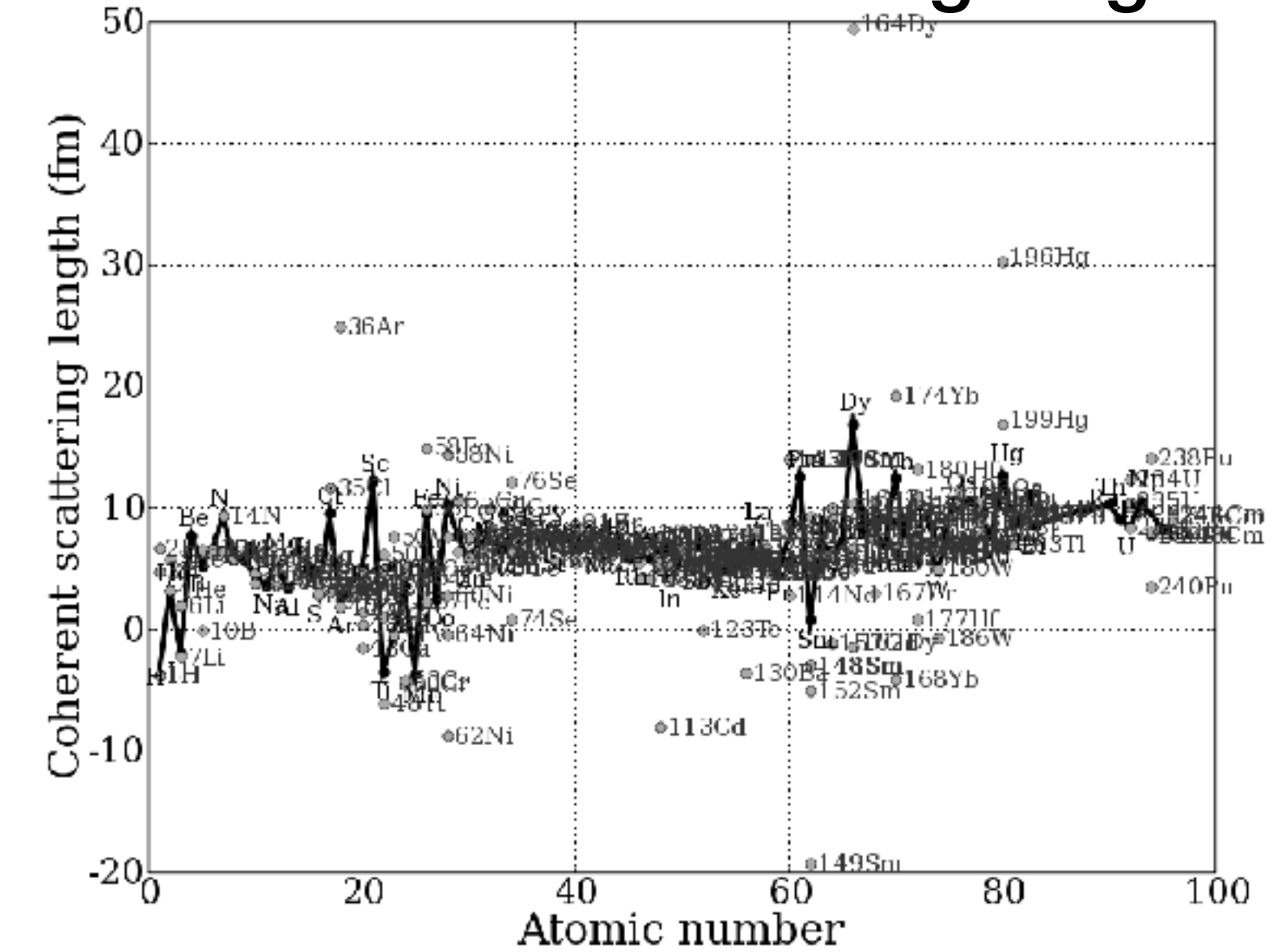
$$2\mu U_{\text{opt}}(r) = -4\pi \left(1 + \frac{\mu}{m}\right) b_0 \rho(r)$$

- $\text{Re } a_0 = (1.54 \pm 0.03) A^{0.311 \pm 0.005} \text{ fm}$
- $\text{Im } a_0 = -(1.00 \pm 0.04) \text{ fm}$



Batty et al., Nucl. Phys. A 689 (2001) 721

cf. neutron scattering length



GISAXS Community Website

- Absence of low-energy scattering measurement

Neutron-antineutron oscillation

- violates both B and B-L (B: baryon number, L: lepton number)
- test of Grand Unified Theory

- Lower limit of oscillation time

- ▷ ILL (1994) free neutron

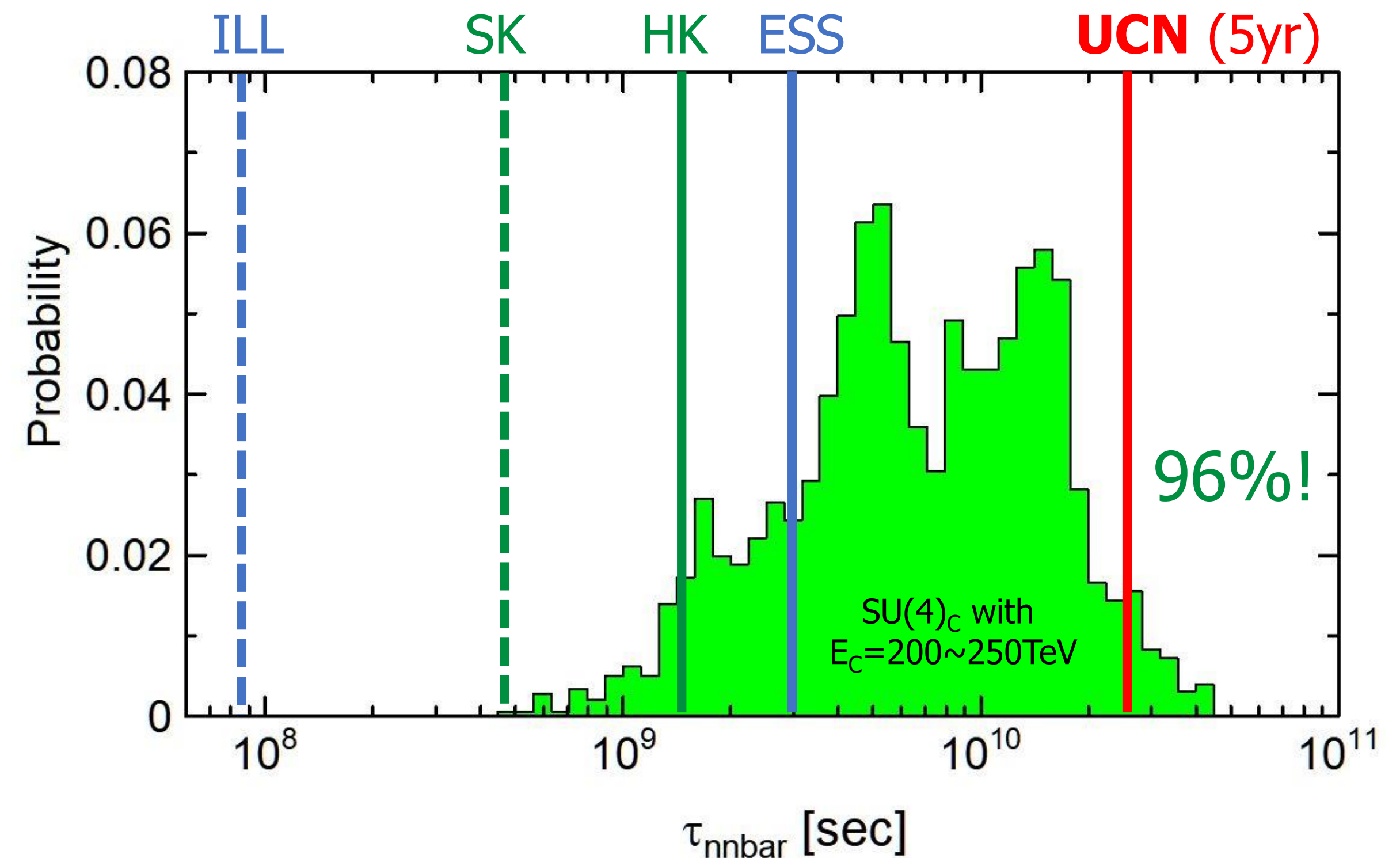
$$\tau_{n\bar{n}} > 8.6 \times 10^7 \text{ s}$$

- ▷ Super-Kamiokande (2021) bound n

$$\tau_{n\bar{n}} > 4.7 \times 10^8 \text{ s}$$

M. Baldo-Ceolin et al., Z. Phys. C 63, 409 (1994).

K. Abe et al., Phys. Rev. D 103, 012008 (2021).



D.G. Phillips II et al., Phys. Rep. 612 (2015) 1

K.S. Babu et al., Phys. Rev. D 87 (2013) 115019

T. Shima, RCNP NEWS Colloquium (2023)

Importance of antineutron-nucleus scattering length

Theoretical analysis of antineutron-nucleus data needed for antineutron mirrors in neutron-antineutron oscillation experiments

K. V. Protasov¹, V. Gudkov², E. A. Kupriyanova³, V. V. Nesvizhevsky⁴, W.M. Snow⁵ and A. Yu. Voronin³

¹Laboratoire de Physique Subatomique et de Cosmologie, UGA-CNRS/IN2P3, Grenoble 38026, France

²Department of Physics and Astronomy, University of South Carolina, South Carolina 29208, USA

³P.N. Lebedev Physical Institute, 53 Leninsky prospect, Moscow 119991, Russia

⁴Institut Max von Laue–Paul Langevin, 71 avenue des Martyrs, Grenoble 38042, France

⁵Department of Physics, Indiana University, 727 East Third Street, Bloomington, Indiana 47405, USA

(Received 10 September 2020; accepted 25 September 2020; published 21 October 2020)

The values of the antineutron-nucleus scattering lengths, and, in particular, their imaginary parts, are needed to evaluate the feasibility of using neutron mirrors in laboratory experiments to search for neutron-antineutron oscillations. We analyze existing experimental and theoretical constraints on these values with emphasis on low- A nuclei and use the results to suggest materials for the neutron-antineutron guide and to evaluate the systematic uncertainties in estimating the neutron-antineutron oscillation time. As an example, we discuss a scenario for a future neutron-antineutron oscillation experiment proposed for the European Spallation Source. We also suggest future experiments which can provide a better determination of the values of antineutron-nuclei scattering lengths.

mirror reflection Phys. Rev. D 102 (2020) 075025

A new approach to search for free neutron-antineutron oscillations using coherent neutron propagation in gas

V. Gudkov^{a,*}, V.V. Nesvizhevsky^b, K.V. Protasov^c, W.M. Snow^d, A.Yu. Voronin^e

^a Department of Physics and Astronomy, University of South Carolina, SC, 29208, USA

^b Institut Max von Laue – Paul Langevin, 71 avenue des Martyrs, Grenoble, 38042, France

^c Laboratoire de Physique Subatomique et de Cosmologie, UGA-CNRS/IN2P3, Grenoble, 38026, France

^d Department of Physics, Indiana University, 727 E. Third St., Bloomington, IN, 47405, USA

^e P.N. Lebedev Physical Institute, 53 Leninsky prospect, Moscow, 119991, Russia

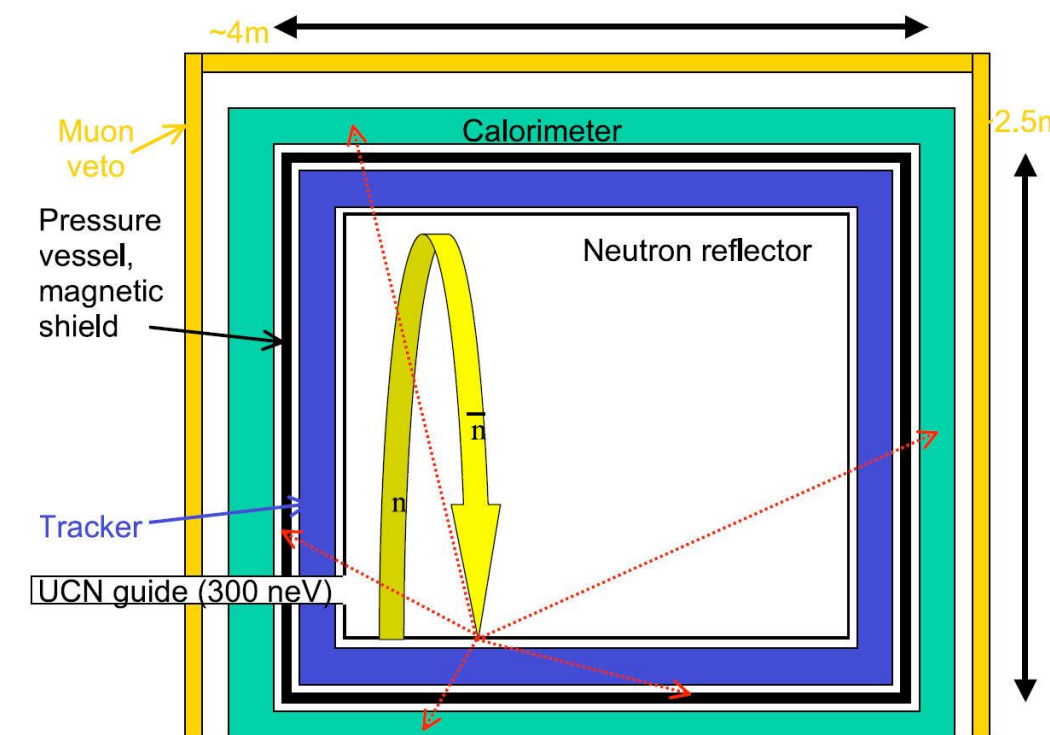
The arguments of this paper apply also to the low energy s -wave scattering of neutrons and antineutrons, and we can apply neutron optics theory to the propagation of antineutrons in gases as well. The value of the neutron index of refraction can be written

gas propagation Phys. Lett. B 808 (2020) 135636

Fermi pseudo-potential

$$U = \frac{2\pi\hbar^2 n}{m_n} a$$

n : number density
 a : scattering length



D.G. Phillips II et al., Phys. Rep. 612, 1-45 (2016)

However...

Inside wall;

$$i \frac{\partial}{\partial t} \begin{pmatrix} \psi_n(t) \\ \psi_{\bar{n}}(t) \end{pmatrix} = \begin{pmatrix} E_n - i\Gamma_\beta/2 + U_n(t) & \varepsilon \\ \varepsilon & E_n - i\Gamma_\beta/2 + U_n(t) \end{pmatrix} \begin{pmatrix} \psi_n(t) \\ \psi_{\bar{n}}(t) \end{pmatrix}$$

where $\omega_w \equiv U_n(t) - U_{\bar{n}}(t) = O(10^{-7} [\text{eV}]) \gg \varepsilon < 10^{-22} [\text{eV}]$

$$v \equiv \frac{1}{2} \sqrt{\omega_w^2 + 4\varepsilon^2} \quad \left(\cong \frac{1}{2} \omega_w, \text{ if } \varepsilon \text{ is extremely small} \right)$$

$$\begin{pmatrix} \psi_n(t_w) \\ \psi_{\bar{n}}(t_w) \end{pmatrix} = \exp \left[- \left(iE_n + \frac{\Gamma_\beta}{2} \right) t_w \right] \cdot \begin{pmatrix} \cos v t_w + \frac{i\omega_w}{2v} \sin v t_w & -\frac{i\varepsilon}{v} \sin v t_w \\ -\frac{i\varepsilon}{v} \sin v t_w & \cos v t_w - \frac{i\omega_w}{2v} \sin v t_w \end{pmatrix} \begin{pmatrix} \psi_n(0) \\ \psi_{\bar{n}}(0) \end{pmatrix}$$

$$\varepsilon \sim 10^{-25} [\text{eV}], \quad v \cong \frac{1}{2} \omega_w \sim 10^{-7} [\text{eV}], \quad t_w \sim 10^{-8} [\text{s}] = 1.5 \times 10^7 [\text{eV}^{-1}]$$

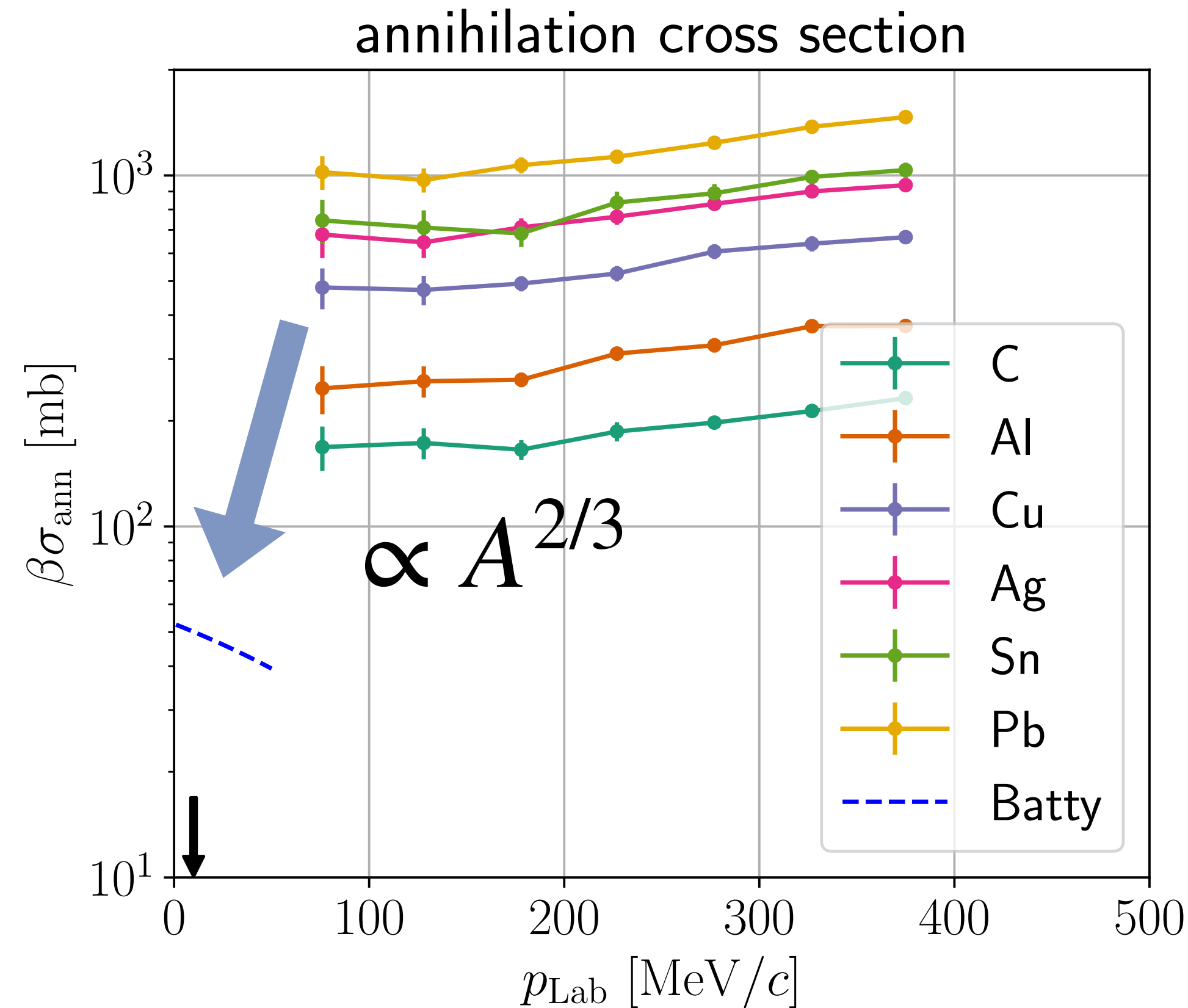
$$\Rightarrow v t_w \cong 1.5$$

$$\Rightarrow \mathbf{R} = \begin{pmatrix} 0.0707 + 0.9975i & 0 \\ 0 & 0.0707 - 0.9975i \end{pmatrix} = 0.0707\mathbf{I} + 0.9975i\sigma_3$$

UCN trap wall Shima (2023)

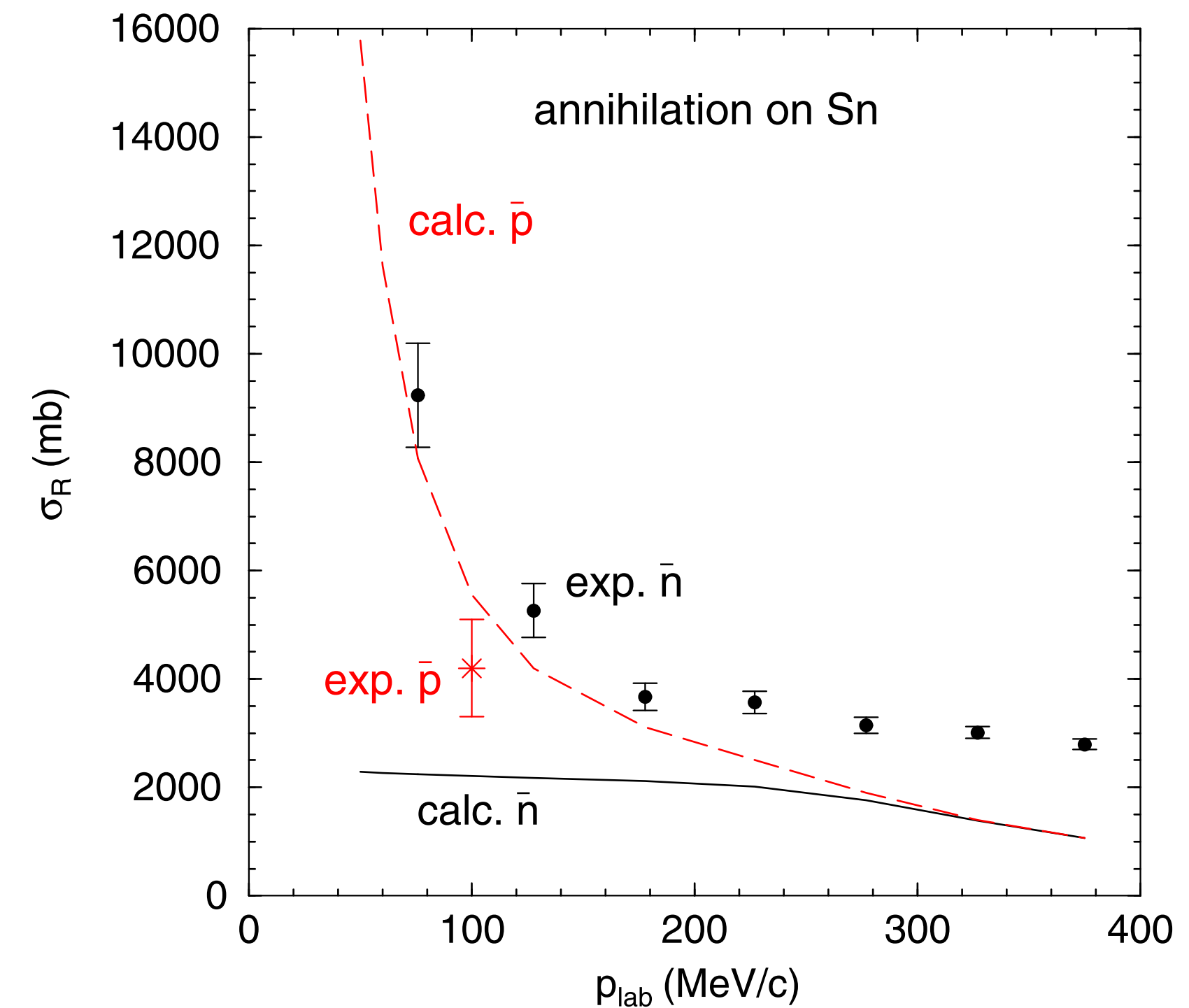
Expected annihilation cross sections

Batty: $a_0 = (1.54 \pm 0.03)A^{0.311 \pm 0.005} - i(1.00 \pm 0.04) \text{ fm}$



NPA 697 (2002) 209

discrepancy between exp. cross sections and calculations using the optical potential which reproduce \bar{p} -atomic levels.



Friedman et al., NPA 925 (2014) 141

Conclusion

- Antiproton-nucleus optical potentials (w/o the b_1 term) were investigated with X-ray spectroscopy of **antiprotonic atoms**.
- We will perform X-ray spectroscopy for antiprotonic atoms in Ca isotopes (^{40}Ca , ^{48}Ca) with TES detectors to deduce b_0 and b_1 parameters.
- Antineutron-nucleus (proton) scattering lengths will be determined by **antineutron-nucleus (proton) scattering measurements at low energies**.
- For this purpose, a low-energy antineutron beamline at CERN-AD is proposed.
- Antineutron-nucleus scattering lengths are very important in search of neutron-antineutron oscillation.